INFLUENCE OF CONVECTION ON MICROSTRUCTURE

NAG8 - 753

Sixth Semi-annual Progress Report

15 February 1991 to 15 February 1992

CLARKSON UNIVERSITY

Potsdam, New York 13699-5700

Principal Investigator: Dr. William R. Wilcox
School of Engineering
Center for Crystal Growth in Space
(315) 268-6446; fax 3841

Co-Investigator: Dr. Liya L. Regel
School of Engineering
Center for Gravity Material Science and Applications
(315) 268-7672

Graduate Student Research Assistant:

Mr. John Rydzewski
Department of Chemical Engineering
(315) 268-6657

Introduction

The primary motivation for this research has been to determine the cause for space processing altering the microstructure of some eutectics, especially the MnBi-Bi eutectic. Prior experimental research at Grumman and here showed that the microstructure of MnBi-Bi eutectic is twice as fine when solidified in space or in a magnetic field, is uninfluenced by interfacial temperature gradient, adjusts very quickly to changes in freezing rate, and becomes coarser when spin-up/spin-down (accelerated crucible rotation technique) is used during solidification. Theoretical work at Clarkson predicted that buoyancy driven convection on earth could not account for the two fold change in fiber spacing caused by solidification in space. However a lamellar structure with a planar interface was assumed, and the Soret effect was not included in the analysis. Experimental work at Clarkson showed that the interface is not planar; MnBi fibers project out in front of the Bi matrix on the order of one fiber diameter.

Originally four primary hypotheses were to be tested under this current grant:

A fibrous microstructure is much more sensitive to convection than a lamellar microstructure, which was assumed in our prior theoretical treatment.

An interface with one phase projecting out into the melt is much more sensitive to convection than a planar interface, which was assumed in our prior theoretical treatment.

The Soret effect is much more important in the absence of convection and has a sufficiently large influence on microstructure that its action can explain the flight results.

The microstructure is much more sensitive to convection when the composition of the bulk melt is off eutectic.

As reported previously, we have learned that while a fibrous microstructure and a non-planar interface are more sensitive to convection than a lamellar microstructure with a planar interface, the influence of convection remains too small to explain the flight and magnetic field results. Similarly addition of the Soret effect does not explain the flight and magnetic field results.

Personnel

The second year of this three-year grant ended on August 14, 1990. The third year's continuation funding was not received until October of 1991, a hiatus of 14 months. Without funding, no new graduate students could be started on this project after Miss Seth and Mr. Mohanty completed their theses in 1990.

A few months ago a new graduate student, John Rydzewski, began learning how to prepare the MnBi-Bi eutectic, prepare ampoules, do metallography on solidified MnBi-Bi, etc.

Also joining the project is Dr. Liya L. Regel, formerly director of research on materials processing in space at the Space Research Institute in Moscow. Although she has not yet received pay from this project, she has been advising Mr. Rydzewski. Before leaving Moscow she arranged to have several Mn-Bi samples directionally solidified in the large centrifuge at Star City. These samples had been prepared by another graduate student, Mr. Ramnath Derebail, who was supported by the New York State Center for Advanced Materials Processing at Clarkson University.

Two new graduate students, Mr. and Mrs. Erlich, were recruited and will begin in March or April. He will perform the theoretical computations outlined below and she will do experiments on the influence of perturbing the freezing rate with electric current pulses.

Progress

Mr. Rydzewski's work is discussed here in Appendix A.

1. A paper was published in the Journal of Crystal Growth on "Effect of convection on the microstructure of a lamellar eutectic growing with a stepped interface." It is included here as Appendix B.

2. A paper was published in the Journal of Crystal Growth on "Directional solidification of Pb-Sn eutectic with vibration." It is included here as Appendix C.

3. A paper was written on "The Soret effect in eutectic solidification." It is included here as Appendix D.

4. A paper reviewing prior research on MnBi-Bi solidification was presented at the International Astronautics Federation Congress in Montreal in October. It was accepted for publication and is included here as Appendix E.

5. Several Mn-Bi ampoules were prepared and directionally solidified at high gravity in the large centrifuge at Star City. The samples were sliced, polished and examined in the optical microscope. The microstructures are unusual, but appear to be bismuth-rich. This is indicative of incomplete alloying because of an oxide coating on the manganese feed material. (This problem is very common with new graduate students.) See Appendix A.

6. Several MnBi-Bi eutectic samples were prepared and supplied to scientists at CNRS in France for directional solidification in the large centrifuge at Nantes. See Appendix A.

7. Discussions have been held with Professor Reginald Smith at Queens University in Canada to do directional solidification experiments using their centrifuge. See Appendix A.

Plans

1. Directionally solidify MnBi-Bi eutectic and off-eutectic mixtures in our laboratory and in the French and Canadian centrifuges. Determine the influence of g level and melt composition on the microstructure. See Appendix A.

2. Determine theoretically the influence of convection on the microstructure of off-eutectic mixtures using a linear velocity gradient in the melt and a planar interface.

3. Complete an examination of the influence of physical properties on the reported changes in eutectic microstructure caused by solidification in space.

4. Determine the influence on the MnBi-Bi microstructure caused by perturbing the freezing rate with electric current pulses.

APPENDIX A

INFLUENCE OF GRAVITY AND COMPOSITION ON Mn-Bi MICROSTRUCTURE

John Rydzewski

Summary

During this period, the research on the effect of convection on the microstructure of the MnBi/Bi eutectic involved:

(a) Preparing and conducting eutectic and off-eutectic experiments in normal earth's gravity.

(b) Planning and preparing eutectic and off-eutectic experiments for high gravity processing, and analyzing samples solidified in high gravity.

In addition, a paper titled "Influence of Gravity on the Microstructure of the MnBi/Bi Eutectic" reviewing the MnBi/Bi research at Clarkson University was presented at the 42nd Congress of the International Astronautical Federation. It will be published in Acta Astronautica and is given here in Appendix E.

Objective

The objective of this research is to determine the effect of high gravity and deviations from the eutectic composition on the microstructure of MnBi/Bi. It is anticipated that this research will help identify the mechanism responsible for the reduction in MnBi fiber spacing in samples solidified in microgravity. In addition to experimentally testing the hypothesis developed by Favier and deGoer [1], it is anticipated that this work will improve the understanding of the effects of high gravity on crystal growth processes.

Introduction

The primary motivation for this research resulted from the observed differences in the microstructure of the MnBi/Bi eutectic when directionally solidified in space compared to samples processed on earth under otherwise identical conditions [2-6]. The MnBi/Bi eutectic microstructure is characterized as a semi-regular, aligned-rod morphology sensitive to growth conditions. MnBi/Bi alloys were directionally solidified in space during the Apollo-Soyuz Test Project (ASTP), on two Space Processing Application Rocket (SPAR) flights, and on one shuttle flight by Larson and Pirich [2,3,6]. The composition was at the eutectic for the SPAR

experiments and slightly off-eutectic for ASTP. In all the experiments, the spacing between the MnBi fibers of the space-processed MnBi/Bi material was about half the spacing of samples solidified in earth under otherwise identical conditions. Space-grown samples have also shown an increase in permanent magnet properties to greater than 97% of the theoretical maximum. Several mechanisms for the difference in microstructure have been suggested.

Previous investigators at Clarkson University have theoretically and/or experimentally studied the effects of natural and forced convection [7-11], temperature gradient [12], growth rate [13], and thermal diffusion [14,15] on solidification of the MnBi/Bi system.

Favier and deGoer [1] proposed an off-eutectic stagnant film model to account for the influence of gravity on eutectic spacing. Their model uses the Jackson and Hunt expression for off-eutectic (plane front) lamellar spacing written in terms of the eutectic phase fraction [16,17]. Assuming the difference in lamellar spacing λ for solidification in earth from that for low-gravity is due exclusively to the effect of convection on the volume fraction, Favier and deGoer developed an expression relating λ at one-g and zero-g in terms of the volume fraction and characteristics of the phase diagram. Their model predicts a 30 to 50% difference between lamellar spacing at one-g and zero-g for a $\pm$1% deviation from the eutectic for a binary system with a very assymmetrical phase diagram. A positive deviation in compositon is predicted to increase λ while a negative deviation should decrease λ. In the case of melts exactly at the eutectic composition, Favier and deGoer predicted that λ is unaffected by convection.

Barczy et al. [18], through their experiments on solidification of different Al_3Ni-Al alloys in high gravity, concluded that the predictions of the Favier and deGoer model are invalid.

Progress

Normal Earth's Gravity Experimentation

During this period, eutectic and slightly hypo-eutectic samples were prepared and directionally solidified in a vertical Bridgman-Stockbarger (VBS) apparatus in normal earth's gravity, g. The Mn compositions of the hypo-eutectic samples ranged from 0.66 to 0.69 wt% Mn in steps of 0.01 wt% Mn. The reason for these Mn compositions is that the eutectic composition of MnBi/Bi is 0.73 +/- 0.03 wt% Mn. To obtain a slightly off-eutectic alloy, the Mn composition has to lay outside of the range given for the eutectic. Also during this period, a new procedure to ensure that the eutectic composition is obtained for eutectic composition experiments was implemented [19]. This involves examining the microstructure of the alloy after it has been homogenized and

selecting the portions of the material that possess the aligned-rod morphology characteristic of the eutectic. Only these portions are used for solidification experiments. This method is used to confirm that the growth material is at the eutectic composition.

High-Gravity Experimentation

Analysis has begun on samples processed at 1,3,5,7 and 9g in the C-18 centrifuge at Star City in the former Soviet Union. After a first-glance examination of the samples, it has been determined that a thorough photographic inspection of the transverse sections of each sample will be conducted to properly, and more accurately, characterize the microstructures of the samples.

Eutectic samples have also been prepared and delivered for processing to Drs. Williams and Rodot in the C-5.5 centrifuge located in Nantes, France. Three of these samples will be solidified at different growth rates at the same g-level in the Meudon-2 furnace, while one sample will be used as a control and solidified in normal earth's gravity.

Meetings at Queen's University in Kingston, Ontario, between representatives from Clarkson University and Queen's University have led to access to the Queens centrifuge for solidication of our samples at high-gravity.

Plans

Normal Earth's Gravity Experimentation

Future work will involve the analysis of the eutectic and hypo-eutectic samples, and preparing, solidifying, and analyzing the hyper-eutectic samples. The hyper-eutectic samples will have compositions ranging from 0.76 to 0.79 wt% Mn. If deemed necessary and/or if time permits, further experimentation with additional off-eutectic samples will be conducted.

The translation rate of the ampoule into the cold zone of the vertical Bridgman-Stockbarger apparatus will be 30 mm/hr. The actual freezing rate will be measured by current interface demarcation.

High Gravity Experimentation

Preparations for high-gravity experimentation at Queen's University will continue. It is planned that eutectic and slightly off-eutectic MnBi/Bi alloys will be directionally solidified at 1,3,5,7, and 9g. These gravity levels were chosen because samples were solidified at these levels in the C-18 centrifuge at Star City.

Also, we hope to use current interface demarcation to study the changes, if any, in the interface shape of eutectic samples solidified in a high-gravity environment. This work is contingent upon the feasibility of incorporating the interface demarcation apparatus into the centrifuge furnace configuration.

References

[1] J.J Favier and J. deGoer,in *5th European Symposium on Material Science Under Microgravity, ESA SP-222*, Scholss Elmau, Germany (1984).

[2] R.G. Pirich and D.J. Larson in G.E. Rindone, editor, *Materials Research Society, Annual Meeting*, p 523 (1982).

[3] R.G. Pirich, D.J. Larson and G. Busch, *AIAA J.* 19 (1981) 589.

[4] J. Bethin, "SPAR X Technical Report for Experiment 76-22. Directional Solidification of Magnetic Composites," Report RE-691, Grumman Aerospace Corporation (1984).

[5] J.L. DeCarlo and R.G. Pirich, "Thermal and Solutal Convection Damping Using an Applied Magnetic Field," Report RE-680, Grumman Aerospace Corporation (1984).

[6] R.G. Pirich and D.J. Larson, "SPAR VI Technical Report for Experiment 76-22. Directional Solidification of Magnetic Composites," Report RE-602, Grumman Aerospace Corporation (1980).

[7] S. Chandrasekhar, G.F. Eisa and W.R. Wilcox. *J. Crystal Growth* 76 (1986) 485-488.

[8] V. Baskaran and W.R. Wilcox. *J. Crystal Growth* 67 (1984) 343.

[9] R. Caram, S. Chandrasekhar and W.R. Wilcox. *J. Crystal Growth* (1990) 294-302.

[10] G.F. Eisa, W.R. Wilcox and G. Busch. *J. Crystal Growth* 78 (1986) 159-174.

[11] J. Seth, M.S. Thesis, Clarkson University (1990).

[12] P.S. Ravishankar, Ph.D. Thesis, Clarkson University (1980).

[13] W.R. Wilcox, K. Doddi, M. Nair and D.J. Larson. *Adv. Space Res.* 3 (1983) 79-83.

[14] A.P. Mohanty, M.S. Thesis, Clarkson University (1990).

[15] R. Caram and W.R. Wilcox, "Influence of Convection on Microstructure," Third Semi-Annual Progress Report, NAG8-753, Clarkson University (1990).

[16] J.D. Verhoeven and R.H. Homer. *Met. Trans.* 1 (1970) 3437.

[17] K.A. Jackson and J.D. Hunt. *AIME Trans.* 236 (1966) 1129.

[18] P. Barczy, J. Solyom and L.L. Regel in *First International Workshop on Materials Processing in High Gravity*, Dubna, USSR (1991).

[19] O. Radkevich. Private Communication, Queen's University (1991).

Original (Copy 3)

THE SORET EFFECT IN EUTECTIC SOLIDIFICATION

R. Caram* and W.R. Wilcox

Clarkson University, Potsdam, NY 13699-5700, USA

ABSTRACT

In eutectic growth, as the solid phases grow they reject atoms to the liquid. This results in a variation of melt composition along the solid/liquid interface. In the past, mass transfer in eutectic solidification, in the absence of convection, was considered to be governed only by the diffusion induced by compositional gradients. However, mass transfer can also be generated by a temperature gradient. This is called thermotransport, thermomigration, thermal diffusion or the Soret effect.

This paper presents a theoretical model of the influence of the Soret effect on the growth of eutectic alloys. A differential equation describing the compositional field near the interface during unidirectional solidification of a binary eutectic alloy was formulated by including the contributions of both compositional and thermal gradients in the liquid. A steady-state solution of the differential equation was obtained by applying appropriate boundary conditions and accounting for heat flow in the melt. Following that, the average interfacial composition was converted to a variation of undercooling at the interface, and consequently to microstructural parameters.

The results obtained show that thermotransport can, under certain circumstances, be a parameter of paramount importance.

* Permanent address: State University of Campinas, Brazil

1. INTRODUCTION

Directional solidification applied to growth of eutectic alloys is one of the most efficient techniques to produce composite materials. In-situ composites obtained by this process typically have a notable degree of thermal stability and better properties than their individual constituents. Eutectic and eutectoid growth has been the topic of several theoretical studies since it was first studied by Zener [1] and Brandt [2]. Following these basic works, the mathematical modeling of eutectic solidification was discussed many times, including the classical work of Jackson and Hunt [3].

Recently several investigators have studied the directional solidification of eutectic alloys in space. Since microgravity greatly decreases buoyancy driven convection, eutectic solidification under such conditions is expected to result in a pure diffusion-controlled growth. During experiments on directional solidification of MnBi-Bi eutectic in the space environment, the microstructure obtained was finer than when solidification was done on earth under otherwise identical conditions [4-6]. Apparently, these results were due to reduced convection in space. Theoretical work, considering a convective flow across the interface, led to the prediction that convection during solidification coarsens an eutectic microstructure by changing the composition of the interfacial liquid [7-10]. However, the results showed that natural convection on earth is not sufficient to cause the finer microstructure observed in low gravity processed samples [11].

A reasonable hypothesis for the low gravity change in eutectic microstructure involves thermal diffusion during directional solidification. The thermal diffusion phenomenon, also known as the Soret effect, is the relative separation of the constituents of a mixture while it is held in a thermal gradient in the absence of convection [12]. In a vertical column, this separation leads one of the components to migrate upward or downward, depending on the sign of the Soret coefficient. The Soret coefficient depends on temperature, pressure and concentration [13]. The separation caused by thermomigration is dissipated by convected motion of the fluid.

During the growth of a eutectic alloy, as the solid phases are formed they segregate atoms into the liquid. This segregation causes a change in the interfacial liquid composition and, thereby, determines the eutectic microstructure [3]. When thermal diffusion occurs

during eutectic solidification, it is expected to induces a variation in liquid composition near the freezing interface. This change may cause a significant modification in microstructure. Even a small amount of fluid convection may be sufficient to eliminate the interfacial composition change produced by the Soret effect.

The purpose of this work is to develop a mathematical model to describe the influence of the Soret effect during the growth of dilute eutectic alloys in the absence of convection.

2. MATHEMATICAL MODEL

Consider the unidirectional solidification of a molten dilute eutectic binary alloy at steady-state [14]. As the solid/liquid transformation proceeds, two solid phases are grown and the average composition of the frozen solid is the same of the liquid far from the interface, here taken to be the eutectic composition C_E.

In order to start this analysis, an interfacial mass balance, similar to the one developed by Yue [15,16], was done. According to figure 1, in the absence of convection for one dimensional behavior the liquid composition $C(z)$ is influenced by three factors:

a. Flux due to the compositional gradient:

$$J_1 = -D\frac{\partial C}{\partial z} \tag{1}$$

b. Flux due to the advancing solid/liquid interface:

$$J_2 = -VC \tag{2}$$

c. Flux due to the temperature gradient for a dilute alloy:

$$J_3 = -D'C\frac{\partial T}{\partial z} \tag{3}$$

where D' is the thermal diffusion coefficient and D is the usual molecular diffusion coefficient. Henceforth both D' and D are assumed to be constant with respect to temperature and concentration. Here V is the rate of displacement of the interface, $\partial T/\partial z$ is the temperature gradient in the liquid at the interface, $\partial C/\partial z$ is the gradient of concentration of solute in the liquid at the interface, and z is the distance into the melt from the interface.

The total flux J_T in the z direction is:

$$J_T = J_1 + J_2 + J_3 = -D\frac{\partial C}{\partial z} - VC + D'C\frac{\partial T}{\partial z} \tag{4}$$

Assuming C and T are functions of z only, a mass balance over a differential element in the liquid yields:

$$\frac{\partial C}{\partial t} = -\frac{\partial J_T}{\partial z} = D\frac{\partial^2 C}{\partial z^2} + V\frac{\partial C}{\partial z} - D'(C\frac{\partial^2 T}{\partial z^2} + \frac{\partial T}{\partial z}\frac{\partial C}{\partial z}) \tag{5}$$

Assuming that the steady-state is reached, $\partial C/\partial t = 0$ and:

$$\frac{\partial^2 C}{\partial z^2} + \frac{V}{D}\frac{\partial C}{\partial z} - \frac{D'}{D}\frac{\partial}{\partial z}(C\frac{\partial T}{\partial z}) = 0 \tag{6}$$

If the composition varies parallel to the interface as well as normal to the interface, we have similarly in three-dimensions:

$$\nabla^2 C + \frac{V}{D}\frac{\partial C}{\partial z} - \frac{D'}{D}\frac{\partial}{\partial z}(C\frac{\partial T}{\partial z}) = 0 \tag{7}$$

In order to know the thermal diffusion we must determine the temperature profile in the melt. This can be done analytically for a thin rod in the absence of convection. Assuming the temperature is function of z only, a steady-state heat balance over a differential element gives:

$$kR\frac{\partial^2 T}{\partial z^2} + \rho C_p VR\frac{\partial T}{\partial z} + 2h(T_h - T) = 0 \tag{8}$$

where k is the thermal conductivity of the melt, R is the radius of the sample, ρ is its density, C_P is the heat capacity, h is the heat transfer coefficient between the rod and the heater, and T_h is the temperature of the heater. This approach is valid for $hR/k << 1$ and $k/C_P\mu << 1$, where μ is the viscosity of the melt. We non-dimensionalize by assuming T_h is constant and letting $B = hR/k$, $Pe = \rho C_P VR/k$, $\eta = z/R$ and $\Phi = (T-T_h)/(T_0-T_h)$. Then, equation 8 can be written as:

$$\frac{\partial^2 \phi}{\partial \eta^2} + Pe\frac{\partial \phi}{\partial \eta} - 2B\phi = 0 \tag{9}$$

For a long rod, the boundary conditions are:

at $\eta = 0$:

$$\phi = 1 \tag{10}$$

and at $\eta \to \infty$:

$$\phi = 0 \tag{11}$$

The solution of equation 9 is:

$$\phi = \exp[-(\frac{Pe + \sqrt{Pe^2 + 8B}}{2})\eta] \tag{12}$$

or

$$T(z) = T_h + (T_h - T_O)\exp(-\Psi z) \tag{13}$$

where T_O is the temperature of the interface and Ψ is given by:

$$\Psi = \frac{Pe + \sqrt{Pe^2 + 8B}}{2R} \tag{14}$$

From this the temperature gradient in the melt is:

$$\frac{\partial T}{\partial z} = \zeta\exp[-\Psi z] \tag{15}$$

where

$$\zeta = \Psi(T_h - T_E) \tag{16}$$

Substituting equation 15 into equation 7, we obtain:

$$\nabla^2 C + \frac{V}{D}\frac{\partial C}{\partial z} - \frac{D'}{D}\zeta\frac{\partial[C\exp(-\Psi z)]}{\partial z} = 0 \tag{17}$$

To solve equation 17, we use the same boundary conditions at the interface as described by Jackson and Hunt [3]. On the other hand, the appropriate boundary condition far from the interface is not clear. Because the temperature gradient extends far into the melt, the concentration variation also extends far into the melt. Since a numerical solution appears to be necessary, a large domain would present serious computational difficulties. To avoid this problem we recognize that the concentration variation becomes essentially one dimensional at some small distance from the interface. Thus we break our problem into two parts. Far from the interface the variation in concentration is one dimensional and can be found analytically. Near the interface the variation in concentration is three-dimensional and must be found numerically. Where these two domains meet, the concentration and its gradient must be the same for both solutions.

The concentration in the liquid far from the solid/liquid interface is found by solving equation 17 written for one dimensional transport:

$$\frac{\partial^2 \overline{C}}{\partial z^2} + \frac{V}{D}\frac{\partial \overline{C}}{\partial z} - \frac{D'}{D}\zeta\frac{\partial[\overline{C}\exp(-\Psi z)]}{\partial z} = 0 \tag{18}$$

where $\overline{C}$ is the average concentration at position z. The boundary conditions necessary to solve equation 18 during the growth of an eutectic are, as shown in figure 1:

at $z \to \infty$:

$$\overline{C}(z\to\infty) = C_E \tag{19}$$

At $z=0$ the average melt concentration is assumed to be the eutectic:

$$\overline{C}(z=0) = C_E \tag{20}$$

We find by integrating equation 18 twice:

$$\overline{C}(z) = \frac{C_E \frac{V}{D} \int_0^z \exp\left[\frac{V}{D}z + \frac{D'\zeta}{D\Psi}\exp(-\Psi z)\right] dz + C_E \exp\left(\frac{D'\zeta}{D\Psi}\right)}{\exp\left[\frac{V}{D}z + \frac{D'\zeta}{D\Psi}\exp(-\Psi z)\right]} \tag{21}$$

For the three-dimensional numerical solution the boundary condition at the solid/liquid interface ($z=0$) is found by a material balance which takes into account the Soret effect, normal diffusion and flow of melt into the solid (see figure 2).
Then over the α phase:

$$\left(\frac{\partial C}{\partial z}\right)_{z=0} = -\frac{V}{D}(C_i - C_S^{\alpha}) + C_i \frac{D'}{D}\zeta \tag{22}$$

and over the β phase:

$$\left(\frac{\partial C}{\partial z}\right)_{z=0} = -\frac{V}{D}(C_i - C_S^{\beta}) + C_i \frac{D'}{D}\zeta \tag{23}$$

A regular eutectic rod structure repeats itself periodically in both x and y directions. Therefore the computational domain will be a rectangular area as presented in figure 3. (The interface presents a similar structure to the one described in [3]). The fibers (β phase) are located on the corners of a hexagon. Under such a case, the periodic boundary conditions are:

$$C_{x=0} = C_{x=\lambda} \tag{24}$$

and

$$C_{y=0} = C_{y=\sqrt{3}\lambda} \tag{25}$$

To reduce the number of variables, equation 7 was also non-dimensionalized. The scaling variables are $X=x/\lambda$, $Y=y/\lambda$ and $Z=z/\lambda$. The non-dimensional equation is:

$$\nabla^2 W + \Lambda \frac{\partial W}{\partial Z} - \Gamma\Theta \frac{\partial [W \exp(-\Theta Z)]}{\partial Z} = 0 \tag{26}$$

where $W=C/C_E$, $\Lambda=\lambda V/D$ is a rod spacing based Peclet number, $\Gamma=(T_h-T_E)D'/D$ is a Soret parameter and $\Theta=\lambda\Psi$ is a function of Biot and Peclet numbers. For example, for $\lambda=0.001m$ and typical experimental conditions, $\Lambda=0.1$, $\Gamma=20$ and $\Theta=0.003$. These values were obtained from conditions generally found during crystal growth, i.e. Biot number close to 0.25 and Peclet number close to $2.5x10^{-4}$. Based on our prior experience [9,11], we note that lateral disturbances to the concentration are almost completely damped out by $z=3\lambda$. At this position the 3d numerical solution must match the 1d analytical solution, equation 21. Thus from the non-dimensionalized form of equation 21, we obtain the boundary condition at $Z=3$:

$$\overline{W}(3) = \frac{\Lambda \int_0^3 \exp[\Lambda Z + \Gamma \exp(-\Theta Z)] dZ + \exp(\Gamma)}{\exp[\Lambda Z + \Gamma \exp(-\Theta Z)]} \tag{27}$$

At $Z=0$, equation 22 becomes:

$$\left(\frac{\partial W}{\partial Z}\right)_{Z=0} = -\Lambda(W_i - W_S^{\alpha}) + W_i \Gamma\Theta \tag{28}$$

and over the β phase, from equation 23:

$$\left(\frac{\partial W}{\partial Z}\right)_{Z=0} = -\Lambda(W_i - W_S^{\beta}) + W_i \Gamma\Theta \tag{29}$$

The periodicity condition in the x and y directions yields the following boundary conditions:

$$W_{X=0} = W_{X=1} \tag{30}$$

and

$$W_{Y\text{-}0} = W_{Y\text{-}\sqrt{3}} \tag{31}$$

The solution of this set of equations was found by writing equation 26 in an explicit finite difference form, which was solved by using the Successive Over Relaxation Technique. To simulate a rod eutectic structure, the fibers and the matrix were approximated by an array of square elements as described elsewhere [11].

3. RESULTS AND DISCUSSION

Figure 4 presents profiles of average liquid concentration as a function of distance, for several values of Γ, $A=0.1$ and $\Theta=0.003$. The 3d model was applied to calculate the liquid concentration profile for a eutectic concentration $C_E=0.03$. To reduce computational complexities, the mutual solid solubilities of the α and β phases were assumed to be negligible, so that the composition of these phases were equal to 0 and 1, respectively. A three-dimensional plot of the liquid composition at the rod-like eutectic interface is shown in figure 5. In this figure, the difference between the composition over the fibers and the matrix is clear. The concentration of B over the β phase is much lower than over the α phase, which results from the demand of B atoms to form the fibers and vice-versa.

According to Jackson and Hunt [3], the total undercooling ΔT at a solid/liquid eutectic interface is the sum of that arising from the deviation of the liquid composition from the eutectic and that due to the curvature of the interface. Thermal diffusion is expected to change the interfacial liquid composition, and thereby change the rod spacing. Using an approach similar that used to examine the influence of convection [7], the undercooling ΔT at any interfacial position is:

$$\Delta T = K_1(\overline{W_i} - W_E) + \frac{K_2}{\lambda} \tag{32}$$

where $\overline{W} = \overline{C}/C_E$.

The term for the composition change can be represented by two parts:

$$(\overline{W}_i - W_E) = (\overline{W}_i - W_E)_{JH} - \Delta \tag{33}$$

where Δ is the change due to the Soret effect. The subscript *JH* means the composition difference found by Jackson and Hunt in the absence of Soret effect:

$$(\overline{W}_i - W_E)_{JH} = A\Lambda \tag{34}$$

By calculating the average undercooling for each phase and assuming constant total undercooling, $\Delta T = \Delta T_\alpha = \Delta T_\beta$, the constants K_1 and K_2 were found to be:

$$K_1 = \frac{m_\alpha m_\beta}{m_\alpha + m_\beta} \tag{35}$$

and

$$K_2 = \frac{4K_1}{\sqrt{1 - C_E}}\left[\frac{K_\alpha}{m_\alpha} + \frac{K_\beta(1 - C_E)}{m_\beta C_E}\right] \tag{36}$$

where m is the slope of the liquidus line, K_α and K_β are constants relating λ to the undercooling changes due to curvature, as defined in [3]. The value of A is:

$$A = A_\alpha + A_\beta \tag{37}$$

where

$$A_\alpha = 2M \tag{38}$$

and

$$A_\beta = \frac{2(1 - C_E)M}{C_E} \tag{39}$$

M is obtained by [3]:

$$M = \sum_{n=1}^{\infty} \frac{1}{(n\pi)^3} \left[\frac{J_1\left(n\pi\sqrt{1 - C_E}\right)}{J_0(n\pi)} \right]^2 \tag{40}$$

Finally, Δ is written as:

$$\Delta = \Delta_\alpha + \Delta_\beta \tag{41}$$

where the composition difference from the eutectic for each solid phase is given by:

$$\Delta_\alpha = (\overline{W_i^\alpha} - W_E)_{JH} - (\overline{W_i^\alpha} - W_E) \tag{42}$$

and

$$\Delta_\beta = (W_E - \overline{W_i^\beta})_{JH} - (W_E - \overline{W_i^\beta}) \tag{43}$$

By differentiating equation 32 with respect to the rod spacing λ and setting the result equal to zero, the extremum condition is found to be given by [3]:

$$\lambda^2 = \frac{K_2 D}{K_1 A V \left(1 - \frac{D}{AV}\frac{\partial \Delta}{\partial \lambda}\right)} \tag{44}$$

Without thermal diffusion, $\Delta = 0$ and the rod spacing is given by:

$$\lambda_0^2 = \frac{K_2 D}{K_1 A V} \tag{45}$$

Substituting equation 45 into equation 44 results in:

$$\left(\frac{\lambda}{\lambda_0}\right)^2 = \left(1 - \frac{D}{AV}\frac{\partial \Delta}{\partial \lambda}\right)^{-1} \tag{46}$$

The analysis of the numerical results showed that for constant C_E, Γ and Θ , Δ is virtually independent of Λ. Figure 6 presents Δ as a function of Λ for several intensities of thermodiffusion. Examination of the curves in this figure allows one to write:

$$\Delta = \Lambda f(\Gamma) \tag{47}$$

The term $\partial\Delta/\partial\lambda$ in 46 is given by:

$$\frac{\partial\Delta}{\partial\lambda} = \frac{\partial\Lambda}{\partial\lambda} f(\Gamma) + \Lambda \frac{\partial f(\Gamma)}{\partial\Gamma} \frac{\partial\Gamma}{\partial\lambda} \tag{48}$$

Since Γ is independent of λ, the substitution of equation 48 into equation 46, yields:

$$\left(\frac{\lambda}{\lambda_o}\right)^2 = \left[1 - \frac{f(\Gamma)}{A}\right]^{-1} \tag{49}$$

Figure 7 shows numerical results of $f(\Gamma)$ as a function of Γ, for $\Lambda=0.1$ and Θ equal to 0.003 and 0.03. The thermal diffusion phenomenon decreases the changes of the interfacial liquid composition linearly with increase of the thermal diffusion coefficient. The examination of both cases ($\Theta=0.003$ and 0.03), showed that the variation in the melt composition is essentially the same for those values of Θ. Then, apparently the deviation in interfacial composition is only slightly dependent of Θ. This result leads to the hypothesis that changes in the Biot and Peclet numbers, within the range studied, have only small influences on the effect of thermal diffusion on the eutectic microstructure. Figure 8 presents λ/λ_0 as a function of Γ, for $\Theta=0.003$ and $\Theta=0.03$. By increasing the thermal diffusion effect (Γ), the microstructure is expected to become finer. On the other hand, if the sign of the thermal diffusion coefficient is changed (the solute migrates to the coldest end), the microstructure should coarsen. A polynomial fit for λ/λ_0 as a function (Γ) produces:

$$\frac{\lambda}{\lambda_0} = 1 - 1.2x10^{-4}\Gamma + 2.0x10^{-8}\Gamma^2 \tag{50}$$

The influence of the Soret effect on the rod-like structure, using typical experimental values ($\Gamma=10$ $\Theta=0.003$ and $\Lambda=0.1$), shows a variation very small ($\lambda/\lambda_0 \approx 1$) compared to the same process without this effect. The change obtained is not sufficient to explain the finer structure obtained in samples processed in space.

4. CONCLUSIONS

The results obtained during this theoretical analysis show that the presence of thermal diffusion during rod eutectic solidification may change the fiber spacings. This change is due to a change in the liquid composition at the interface. The average interfacial composition varies linearly with the thermal diffusion coefficient. Also, the results show that the influence of thermal diffusion on the eutectic solidification is little affected by the Biot and Peclet numbers within the ranges studied here. With reasonable values of the parameters, we found that the Soret effect is not enough to explain the change obtained in space.

ACKNOWLEDGEMENT

This research was supported by NASA grant NAG8-753. R. Caram was also supported by the Brazilian Agency for Scientific Development (CNPq).

NOMENCLATURE

Parameters

A Jackson-Hunt constant for fiber spacing

B hR/k, Biot number

C Mass fraction of component B (wt%)

C_P Heat capacity (J m^{-3} K^{-1})

D Diffusion coefficient in the melt (m^2 s^{-1})

D' Thermal diffusion coefficient (m^2 s^{-1} K^{-1})

$f(\Gamma)$ $\Delta(\Gamma)/\Lambda$

h Heat transfer coefficient (W m^{-2} K^{-1})

K Constant defined in equation 35 and 36

k Thermal conductivity (W m^{-1} K^{-1})

M Function defined by Jackson and Hunt for the analytical solution of equation 26 [3]

m Slope of the liquidus line (K $wt\%^{-1}$)

Pe $\rho C_P VR/k$, Peclet number

R Radius of the sample (m)

T Temperature in the melt (K)

V Freezing rate (m s^{-1}).

x,y Distances along the solid/liquid interface (m)

X,Y Dimensionless distances along the solid/liquid interface, x/λ and y/λ

z Distance into the melt from the interface (m)

Z Dimensionless distance into the melt from the interface, z/λ

W C/C_E, Dimensionless concentration

Δ $(\overline{W_l^\alpha} - W_E)_{JH} - (\overline{W_l^\alpha} - W_E)$ for α phase and $(W_E - \overline{W_l^\beta})_{JH} - (W_E - \overline{W_l^\beta})$ for β phase

μ Viscosity of the melt (m^2 s^{-1})

ρ Density of the melt (Kg m^{-3})

λ Spacing between the rods (m)

Γ $(T_h - T_E)D'/D$, Soret parameter

Θ $\lambda \Psi$, Thermal decay distance

Λ $\lambda V/D$, Freezing rate based Peclet number

Subscripts and Superscripts

E Eutectic

h Heater

i Interfacial

JH Pure diffusion growth process, as done by Jackson and Hunt.

α Alpha phase

β Beta phase

REFERENCES

[1] C. Zener, AIME Trans. 167 (1946) 550.

[2] W. H. Brandt, J. Appl. Phys. 16 (1945) 139.

[3] K. A. Jackson and J.D. Hunt, Trans. AIME 236 (1966) 1129.

[4] R. G. Pirich and D.J. Larson, in: Materials Processing in Reduced Gravity Environment of Space, Ed. G.E. Rindone (North - Holland, New York, 1982) p. 253.

[5] R. G. Pirich, G. Bush, W. Poit and D.J. Larson, Jr, Met. Trans. 11A (1980) 193.

[6] G. Muller and P. Kyr, in: Proc. 15th European Symp. on Materials Science under Microgravity, Schloss Elmau, Nov. 1984, ESA SP-222, p.141.

[7] V. Baskaran and W.R. Wilcox, J. Crystal Growth 67 (1984) 343.

[8] S. Chandrasekhar, PhD Thesis, Clarkson University, Potsdam (1987).

[9] S. Chandrasekhar, G.F. Eisa and W.R. Wilcox, J. Crystal Growth 78 (1986) 485.

[10] G. F. Eisa and W.R. Wilcox, J. Crystal Growth 78 (1986) 159.

[11] R. Caram, S. Chandrasekhar and W.R.Wilcox, to be published, J. Crystal Growth.

[12] S. R. de Groot, Physica IX 7 (1942) 699.

[13] D. R. Caldwell, J. Phys. Chem. 79 (1975) 17.

[14] A. S. Yue, J. Crystal Growth 42 (1977) 542.

[15] A. S. Yue, J. Phys. Chem. Solids Suppl. 328 (1967) 197.

[16] A. S. Yue and J. T. Yue, J. Crystal Growth 13/14 (1972) 797.

LIST OF FIGURES

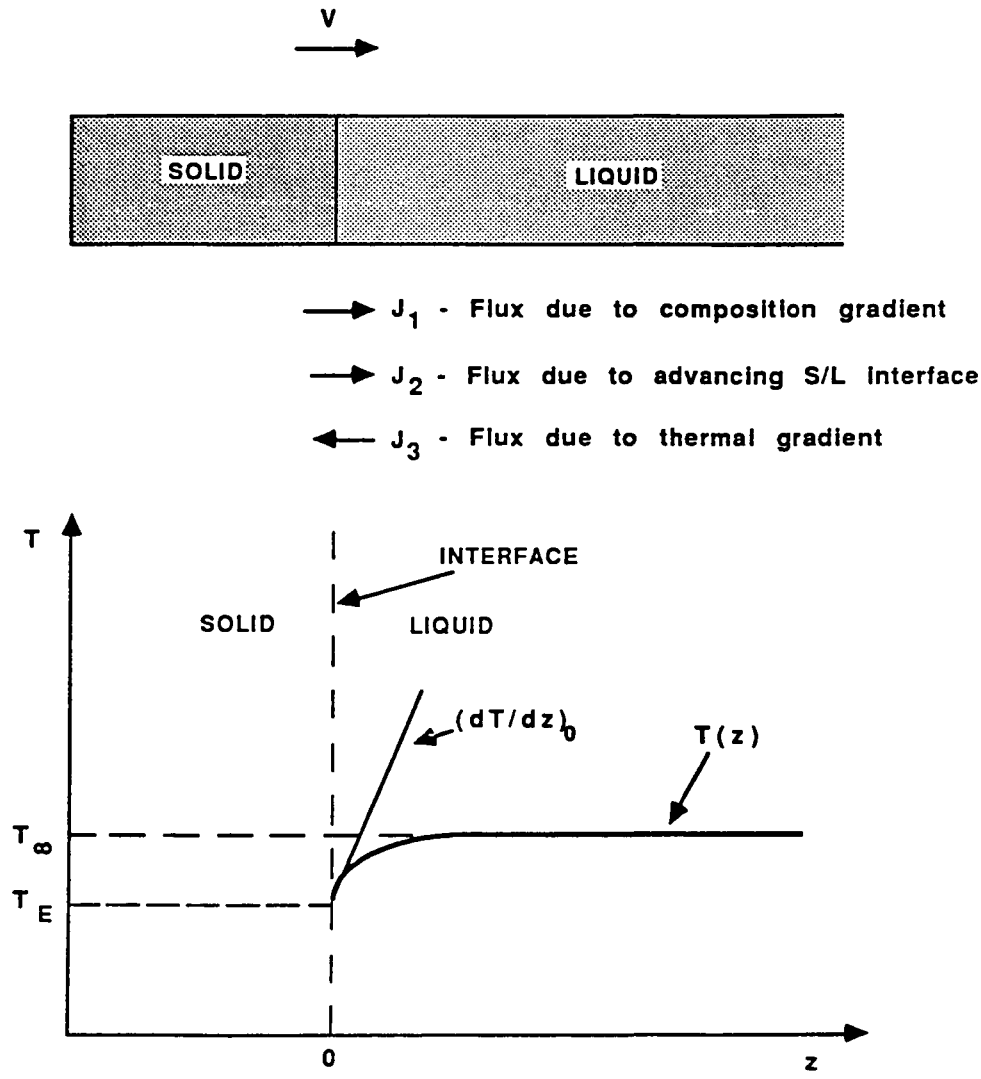
V
SOLID
LIQUID
J1 - Flux due to composition gradient
J2 - Flux due to advancing S/L Interface
J3 - Flux due to thermal gradient
T
INTERFACE
SOLID
LIQUID
(dT/dz)0
T(z)
T∞
TE
0
z

FIGURE 1

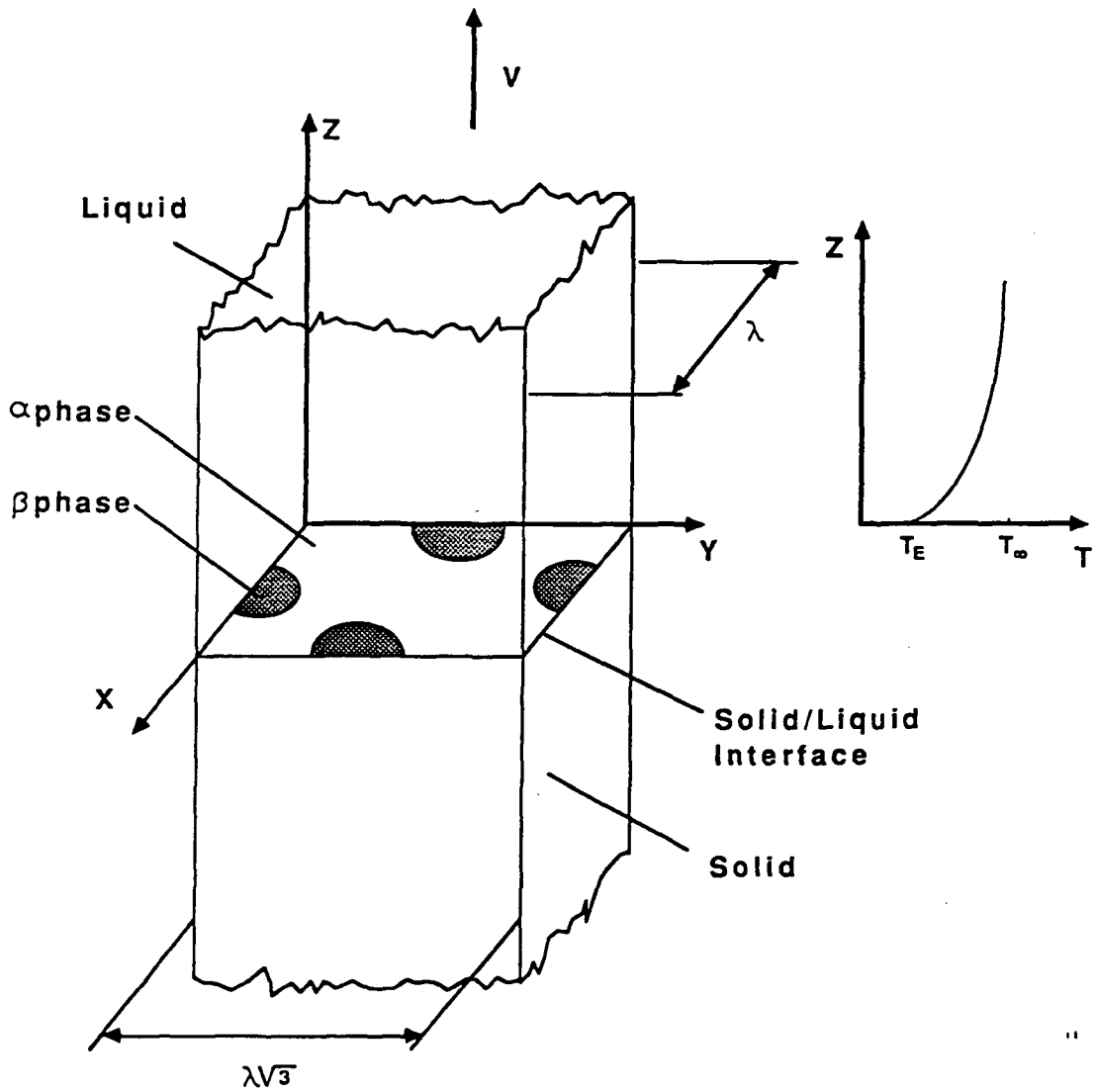
V
Z
Liquid
λ
αphase
βphase
Y
X
Solid/Liquid
Interface
Solid
λV3
Z
T_E
T_∞
T

FIGURE 2

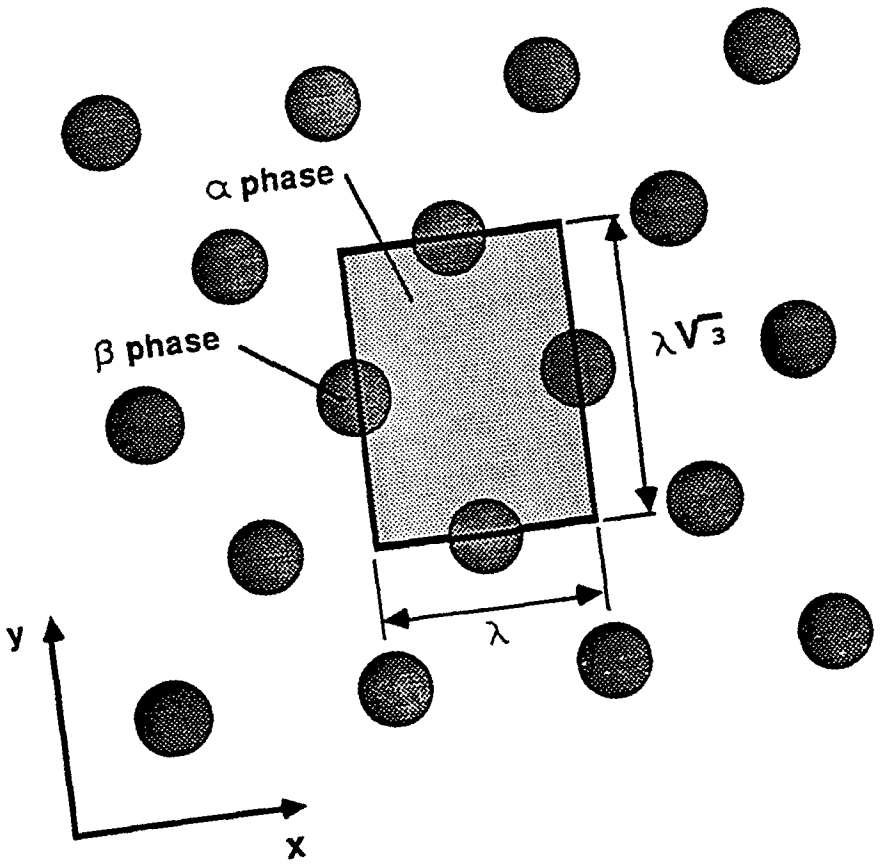

FIGURE 3

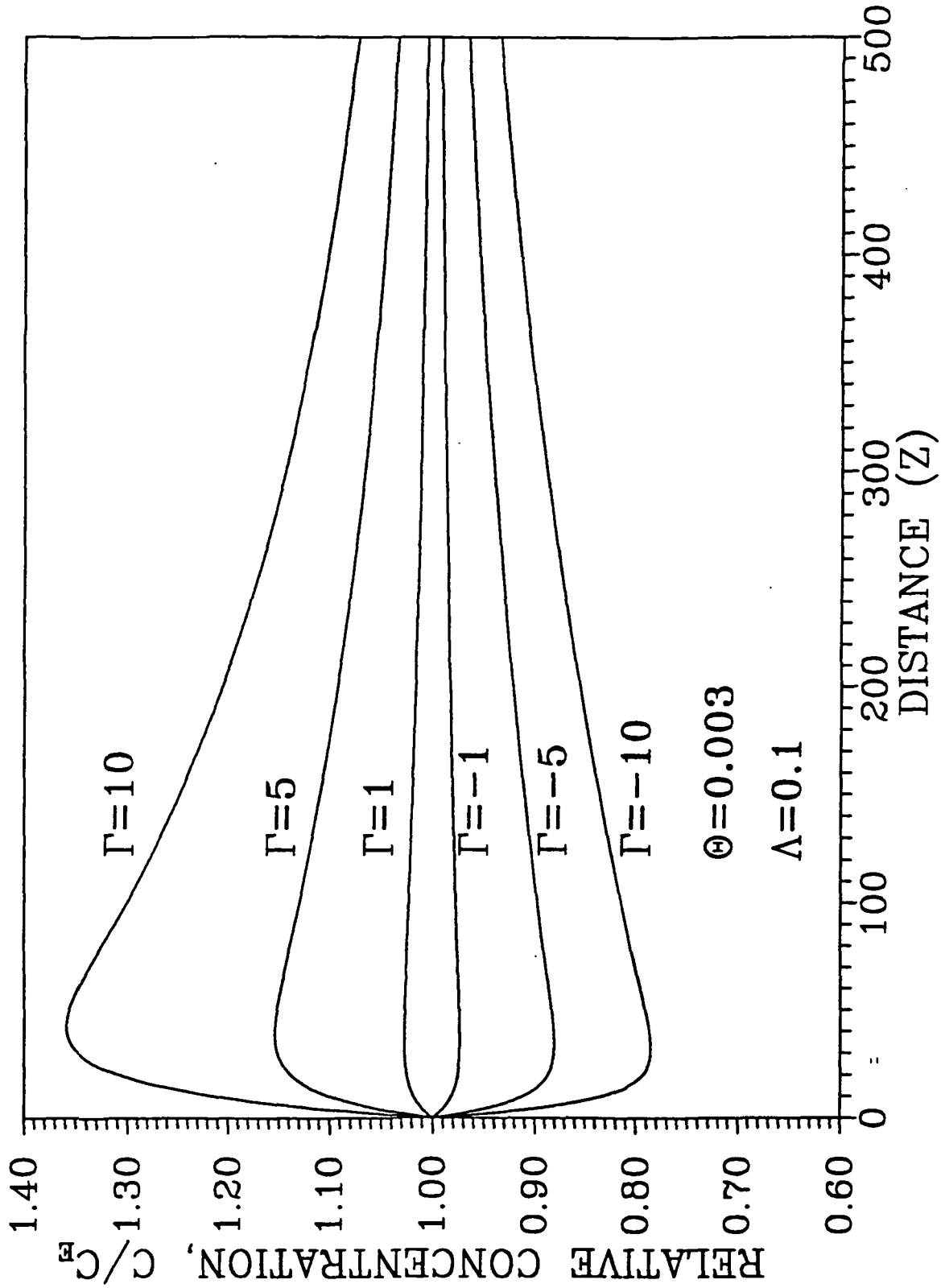
RELATIVE CONCENTRATION, C/C$_E$
1.40
1.30
1.20
1.10
1.00
0.90
0.80
0.70
0.60
0
100
200
300
400
500
DISTANCE (Z)
Γ=10
Γ=5
Γ=1
Γ=-1
Γ=-5
Γ=-10
Θ=0.003
Λ=0.1

FIGURE 4

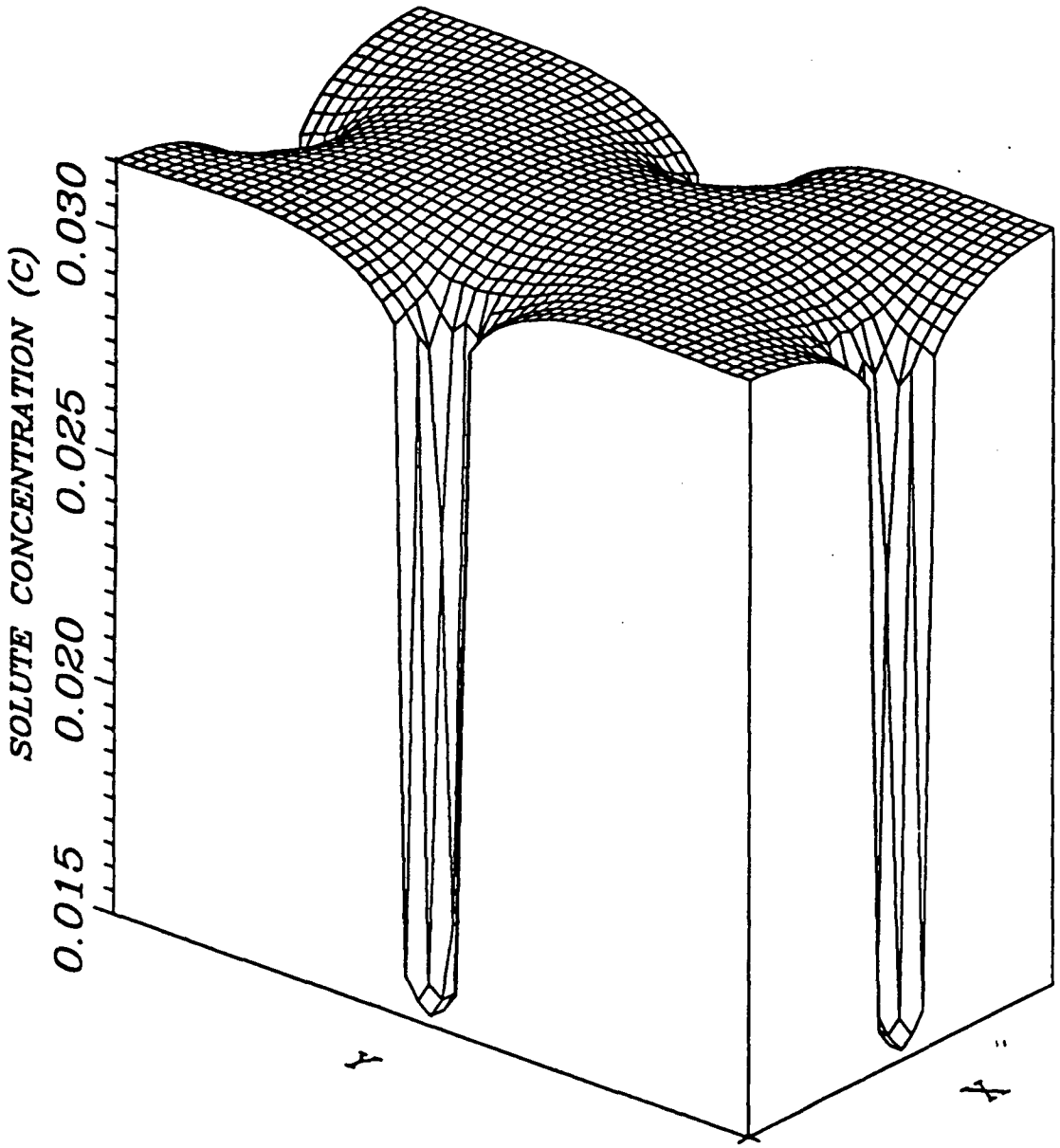

FIGURE 5

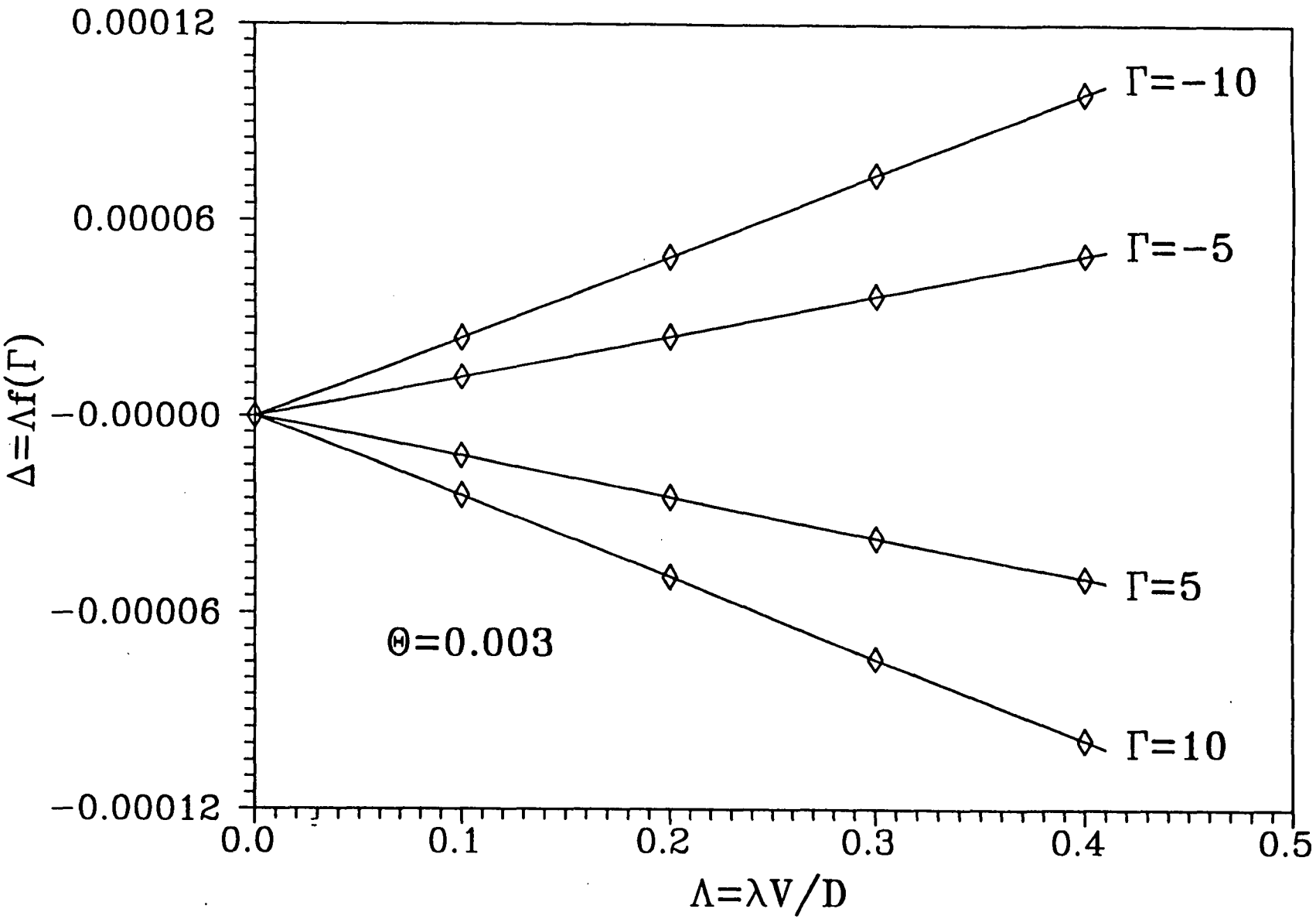
0.00012
0.00006
−0.00000
−0.00006
−0.00012
Δ=Λf(Γ)
0.0
0.1
0.2
0.3
0.4
0.5
Λ=λV/D
Γ=−10
Γ=−5
Γ=5
Γ=10
Θ=0.003

FIGURE 6

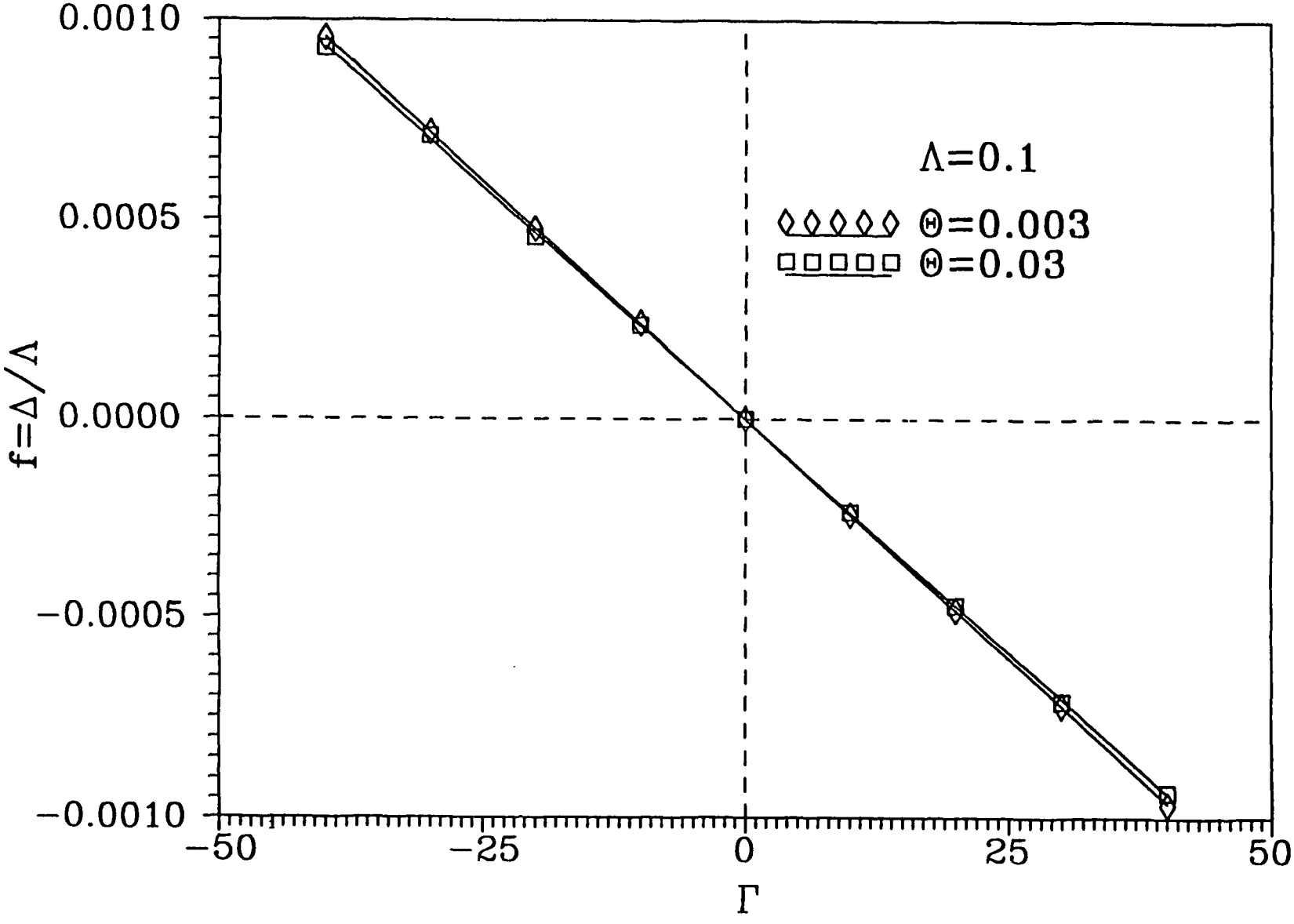
0.0010
0.0005
0.0000
−0.0005
−0.0010
f=Δ/Λ
−50
−25
0
25
50
Γ
Λ=0.1
Θ=0.003
Θ=0.03

Figure 7

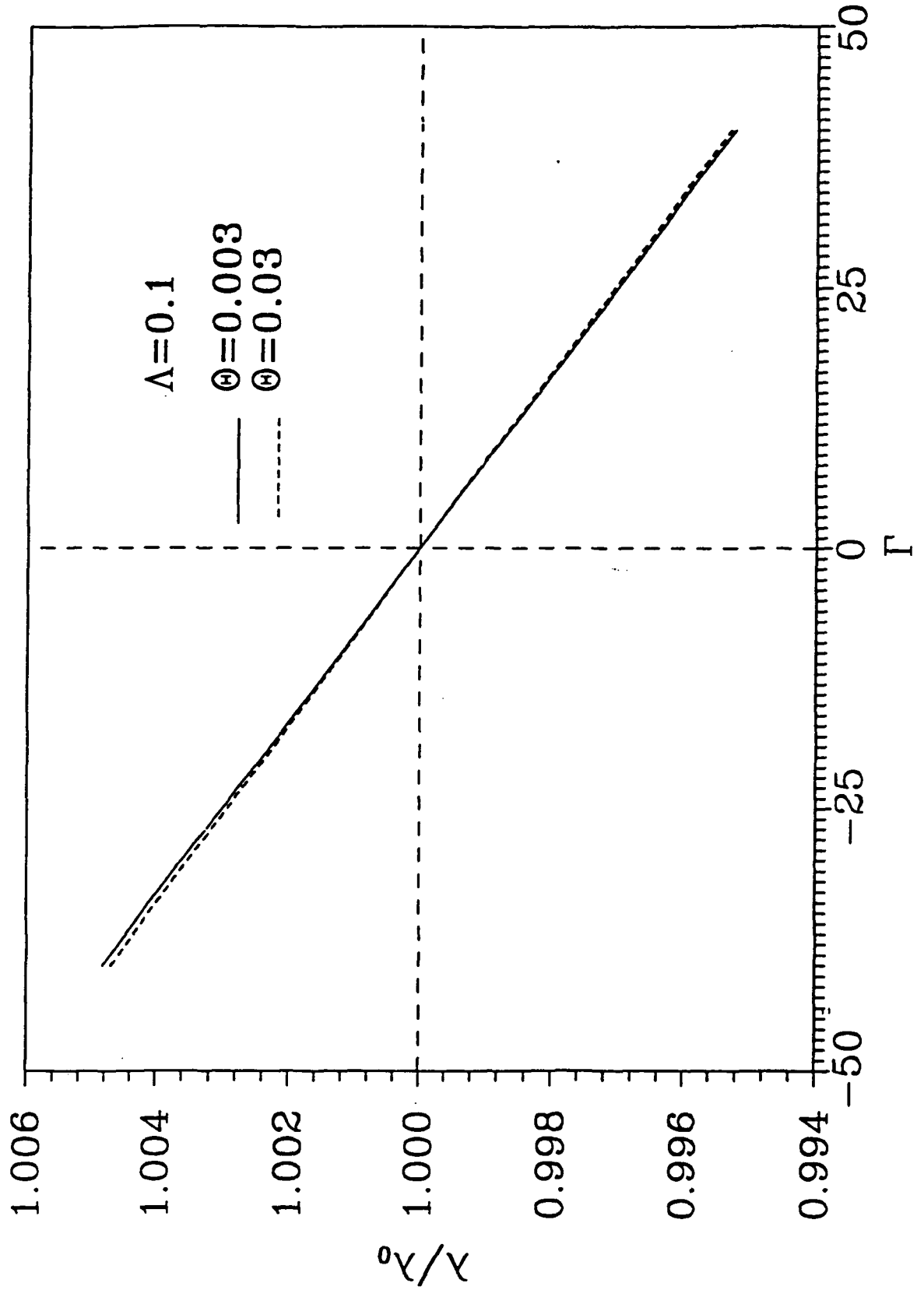
Λ=0.1
Θ=0.003
Θ=0.03
Γ
50
25
0
−25
−50
1.006
1.004
1.002
1.000
0.998
0.996
0.994
λ/λ0

FIGURE 8

APPENDIX E

IAF-91-385

Influence of Gravity on the Microstructure of the MnBi/Bi Eutectic

J.H. Rydzewski and W.R. Wilcox
Center for Crystal Growth in Space
Clarkson University
Potsdam, New York 13699-5700, USA

Abstract

Directional solidification of MnBi/Bi eutectic in space produced MnBi fibers that were significantly finer and closer together than when solidification was carried out on earth under otherwise identical conditions. Use of a strong magnetic field during solidification on earth gave about the same results as solidification in space, indicating that convection is the cause of the difference in microstructure. However, 15 years of theoretical and experimental research have failed to reveal the mechanism for this phenomenon. It has been found that temperature gradient has no effect; the concentration field in front of the freezing interface is not altered sufficiently by buoyancy-driven convection to explain it, even if the MnBi fibers project out in front of the Bi matrix; and the Soret effect is not sufficiently large. On the other hand, vigorous forced convection caused a change in microstructure in agreement with theory.

1. Introduction

Composites have played an important role in filling the demand for materials with more sophisticated mechanical properties that can withstand increasingly severe physical and chemical conditions. Numerous techniques have been developed for the production of composite materials, including directional solidification, which directly yields aligned structures.

Used as a model substance for the study of the rod-like microstructure, the MnBi/Bi eutectic has potential for use in the production of permanent magnets. The eutectic provides a fine dispersion of ferromagnetic particles embedded in a diamagnetic matrix where the MnBi rods are aligned with their easy axis of magnetization parallel to the growth direction in the Bi matrix.

The primary motivation for this research results from the observed differences in the microstructure of the MnBi/Bi eutectic when directionally solidified in space compared to samples processed on earth under otherwise identical conditions. Space-grown samples have also shown an increase in permanent magnet properties to greater than 97% of the theoretical maximum [1-5].

Several mechanisms for the difference in microstructure have been suggested, and previous investigators at Clarkson University have studied the following aspects of the MnBi/Bi eutectic system:

1. Numerical analysis of the effect of convection on the concentration field in the melt ahead of a growing lamellar eutectic interface, and thereby on the microstructure [6-8].

2. Experimental investigation of the effect of forced convection (spin-up/spin-down) on the spacing between MnBi fibers [9].

3. Experimental investigation of the effect of interfacial temperature gradient on the spacing of MnBi rods [10].

4. Experimental investigation of the effect of varying growth rate on the spacing of MnBi rods [11].

5. Numerical model for the influence of convection on a rod-like microstructure [8].

6. Experimental determination of the Soret coefficient of MnBi-Bi melts [12].

7. Numerical analysis of the effect of convection on lamellar spacing of a eutectic growing with a stepped interface [13].

8. Mathematical model for the influence of the Soret effect during growth of eutectic alloys [14].

This paper is a brief review of the progress to date in determining the effect of

gravity on the microstructure of the MnBi/Bi eutectic.

Growth of MnBi/Bi in Space

The microstructure of MnBi/Bi eutectic (0.71 ± 0.03 wt% Mn) is characterized by a regular, aligned-rod morphology that is sensitive to growth conditions. MnBi/Bi alloys were directionally solidified in space during the Apollo-Soyuz Test Project (ASTP) and on two Space Processing Applications Rocket (SPAR) flights by Pirich and Larson [1-5]. The composition was at the eutectic for the SPAR experiments and slightly off-eutectic for the ASTP. In all the experiments, the spacing between the parallel MnBi fibers of the space-processed MnBi/Bi eutectic was about half the spacing of samples solidified on earth under otherwise identical conditions. The results of the microgravity experiments for SPAR and ASTP are summarized in Table 1 and a comparison of the microstructures of earth and space grown samples are in Figure 1.

The MnBi/Bi eutectic, like many other eutectics such as the Al-CuAl [15], Pb-Sn [16-18], and Mg-Al [19], follows the relationship whereby the fiber (or lamellar, see Figure 2) spacing λ is inversely proportional to the square root of the freezing rate V, i.e., $\lambda^2 V$ is constant [10,20,21]. Thus, a 2 to 3 fold reduction in λ corresponds to a 4 to 9 fold increase in V. However, mechanical drive rates were identical for the ground-based and SPAR flights, and no evidence for such an increase in the freezing rate for the space-processed samples was observed.

Besides the MnBi/Bi eutectic, several other eutectics have been solidified in space. Muller and Kyr [22] directionally solidified the InSb-NiSb eutectic on Spacelab-1 and observed a 30% decrease in NiSb fiber spacing compared to earth-grown samples. Favier and deGoer [23] studied the solidification of the Ag-Ge, Al_3Ni-Al and Al_2Cu-Al eutectics in space. When solidified on earth, the Ag-Ge eutectic has an irregular microstructure while Al_3Ni-Al has a fiberlike microstructure and Al_2Cu-Al has a lamellar structure. When solidified in space, only the Al_3Ni-Al was observed to have a major difference in microstructure, whereby the Al_3Ni fibers were spaced farther apart. Carlberg and Sayama [24] observed no differences in microstructure between earth and space-processed samples of the Al_2Cu-Al or Al-Si (fan shaped Si plates in an Al matrix) eutectics while Yue et al. [25] observed that when the NaCl-LiF eutectic was solidified in space, the growth of NaF and LiF fibers in a NaCl matrix was continous and free of kink-bands. The origin of kink-bands in earth-grown samples was attributed to the frequent generation and termination of fibers in the presence of convection currents and vibrations in the melt during growth.

2. Ground-Based Experimentation

Effect of Growth Rate on λ

The theory for the effect of growth rate on a two-phase microstructure was first developed by Zener [21], who stated that:

$$\lambda \propto V^{-0.5}$$

Jackson and Hunt [26] gave a more quantitative treatment of eutectic solidification beginning with a description of the solute diffusion field in front of the growing lamellae. They showed that a rod morphology should grow with a lower undercooling than a lamellar morphology (and therefore should be the stabler growth form) when the volume fraction of one phase is $1/\pi$ for systems with isotropic surface energies. This is in qualitative agreement with observations by Hogan et al. [27]. In an attempt to verify this relationship for the rod microstructure of the MnBi/Bi eutectic, Ravishankar [10] directionally solidified MnBi/Bi in a vertical Bridgman-Stockbarger apparatus at growth rates varying from 0.6 cm/hr to 30 cm/hr. The experimental results were in agreement with the theory, i.e., fiber spacing was proportional to the inverse square root of the freezing rate.

Doddi [28] suggested that a fluctuating growth rate due to convection can perhaps increase λ on earth because the MnBi fibers are faceted and the branching of faceted fibers is difficult. He hypothesized that λ would not respond as quickly to an increasing growth rate as to a decreasing growth rate. The result would be that λ would correspond to a lower growth rate than the average rate, thus resulting in coarser fibers.

Doddi experimentally observed the response of the microstructure of the MnBi/Bi eutectic to step changes in the ampoule translation rate. He observed a gradual response by the microstructure, occurring over approximately 1 cm of ingot length, to sharp changes in the translation rate. He also noted that the fibers did not appear to be uniformly distributed and the fibers on the outermost edge of the cylindrical section were normal to the internal fibers, thus indicating a highly curved interface.

Doddi's proposal called for a faster response by the microstructure to a decrease than to an increase in freezing rate. However, he observed experimentally that the microstructure adjusted as rapidly to a step increase as to a step decrease in ampoule translation rate. This adjustment occurred more rapidly than heat transfer allowed the freezing rate to change. Although Doddi's experimentation did not provide a test of his proposed model to explain the influence of space processing on the microstructure of the MnBi/Bi eutectic, his work did confirm the validity of the theoretical heat transfer model developed by Fu [29,30].

In similar work conducted by Nair [31], disturbances in the growth rate of the MnBi/Bi eutectic were made to see if changes in λ occurred. In addition to the step changes studied by Doddi [28], Nair also studied the evolution of microstructure during a steady decrease in the ampoule translation rate. For step increases in ampoule translation rate, the initial rate was 3.15 cm/hr and was increased to 11.5 cm/hr. Over a distance of 1 cm, Nair observed that the microstructure came to consist of thinner rods spaced closer together. The transition to a different steady state was gradual. Before a rate change was affected, the λ remained constant. In the transition region before the new steady state was achieved, the value of λ decreased. Over the 1 cm transition region, λ reached the new (lower) steady state value. From photomicrographs, she observed several instances of what appeared to be fiber branching in the transition region, and proposed fiber branching is the controlling spacing adjustment step when freezing rate is increased. Nair concluded that branching of faceted MnBi fibers does not occur instantaneously, but with some difficulty. Nair also observed fiber termination occurs much more readily than does fiber branching so that $\lambda^2 V$ is almost equal to the steady state value for a decreasing growth rate, but not for a rapidly increasing freezing rate. She concluded that for the step and gradual decrease in freezing rate, the controlling spacing adjustment mechanism is fiber termination, which appears to respond more readily to the new growth conditions.

Effect of Temperature Gradient on λ

No dependence of temperature gradient on rod spacing was anticipated until Towloui and Hellawell [32] examined the effects of temperature gradient on the microstructure of the Al-Si eutectic. They found that λ was proportional to the inverse square root of the growth rate for a fixed temperature gradient, and that λ was proportional to the inverse cubed root of temperature gradient for a fixed growth rate. In the absence of a model, Toloui and Hellawell speculated that the observed temperature gradient effect should be a general feature of all faceted/non-faceted (f/nf) eutectics. Fisher [33] presented evidence for an increased incidence of branching in organic eutectics at higher interfacial temperature gradients, leading to smaller λ values. He proposed that the faceted morphology of fibers decreases their flexibility to adjust their spacing to local

changes in growth conditions. Therefore, Fisher stated, the rod spacing continues to increase until a 'catastrophic' incident, such as branching, occurs. He termed this 'branching limited growth' and developed a mechanism whereby at higher temperature gradients, branching is made easier. Fisher's theory stated that growth anisotropy of faceted fibers results in the inability to optimize spacing, and therefore concluded his theory valid for all f/nf systems.

Ravishankar [10] varied the interfacial temperature gradient from 5°C/cm to 90°C/cm for the f/nf MnBi/Bi eutectic and, contrary to Fisher and Towloui and Hellawell, determined that the temperature gradient does not have influence over λ for this system.

Effect of Convection on λ

DeCarlo and Pirich [34] directionally solidified the MnBi/Bi eutectic in a Bridgman-Stockbarger furnace in the presence of a static, homogenous, transverse magnetic field to quench buoyancy-driven convection and to stop the concomitant temperature fluctuations [35,36]. They observed that in a field of 3000 gauss, the microstructure and sample properties for samples grown at freezing rates larger than 3 cm/hr, as well as changes in undercooling during solidification [37] in the magnetic field were similar to the results of low-gravity experiments. This indicates that the space environment changes λ by reducing buoyancy-driven convection for eutectoid phase transitions [21].

The accelerated crucible rotation technique (ACRT) is the term used by crystal growers for spin-up/spin-down, the term used by the fluid mechanics community. It is being increasingly used to produce forced convection to stir melts during the growth of crystals. Spin-up refers to processes that occur when the angular velocity of a cylinder filled with a fluid is increased. Spin-down occurs when the angular velocity is decreased or brought to rest. ACRT involves alternating the spin-up and spin-down of the fluid. Rotating the crucible at a constant rate results in rigid body rotation of a homogenous fluid and does not lead to any mixing, although it does help to even out temperature asymmetry due to the heating method used. On the other hand, ACRT results in good mixing near the crystal-melt interface. ACRT has been used to grow good quality crystals of oxides by flux growth [38-41] and $Hg_xCd_{1-x}Te$ by directional solidification [42]. It also proven useful in preventing interface breakdown in Czochralski growth of metallurgical grade silicon [43].

Eisa [44] studied the influence of ACRT on the microstructure of the MnBi/Bi eutectic and discovered that at low freezing rates, increased spin-up/spin-down coarsened the microstructure and caused a deviation in the volume fraction of MnBi from the eutectic composition. Eisa also noted that the interphase spacing of the MnBi/Bi eutectic increased with increasing radial position. For small freezing rates, stirring caused the MnBi to be absent from the center of the ingot. Since MnBi has a lower density than Bi, one cannot invoke centrifugal force throwing out solid MnBi floating in the melt. At intermediate freezing rates, stirring caused a change in morphology of the MnBi from fibrous to degenerative platelets, and coarsening of the microstructure persisted to moderately high freezing rates.

Chandrasekhar [45] observed that MnBi/Bi eutectic solidified at 0.25 cm/hr with 100 rpm spin-up/spin-down had a microstructure consisting of a central core of small irregular rods of MnBi and an outer ring of broken blades. This microstructure was sensitive to heater and cooler temperatures, presumably because of changes in the interface shape. At growth rates greater than 4.8 mm/hr, ACRT did not have any observable effect on the finer spacing. Schematics of these results can be seen in Figure 3. Chandrasekhar confirmed the previously observed trends [7-9] that vigorous convection increases the lamellar spacing, however, the observed changes in

the microstructure were not enough to explain the difference between earth and space-processed samples.

Decanting Experiments

Although optical microscopy is a powerful tool for investigating the microstructure, it suffers from the fundamental limitation that any conclusions regarding the three-dimensional microstructure of the eutectic must be based on inferences from two-dimensional sections. Thus, valid judgments regarding the nature of branching of the MnBi fibers are not possible from an examination of these sections. Etching to selectively remove the Bi matrix of the MnBi-Bi eutectic to free the fibers was attempted without success at both Grumman Corporation and Clarkson University [45].

Decanting provided three-dimensional views of short lengths of MnBi fibers by interrupting solidification and pouring off the remaining melt [45]. Chandrasekhar established that MnBi fibers project ahead of the bismuth matrix during solidification (Figure 4). The amount by which these fibers projected out into the melt varied widely for a given sample. The average ratio of the length projecting out to the fiber diameter, 1/d, is given in Table 2 for different solidification conditions.

Chandrasekhar proposed that with no convection present, solidification of the MnBi/Bi eutectic occurs by coupled growth of the MnBi fibers and the Bi matrix with a near planar interface. Growth without the disturbing influence of convection could be assumed to occur at the extremum, i.e., with minimum undercooling. On the other hand, irregular convection might cause the interface to occasionally melt back. If the kinetics of melting of the Bi matrix is faster than that of the MnBi fibers, the MnBi fibers would project out of the matrix throughout the solidification process.

Soret Effect Measurements

The Soret effect, or thermal diffusion, is the relative movement of components in a mixture due to an applied temperature gradient. In the absence of convection, the Soret effect alters the concentration field in the melt via the separation of components, and therefore, according to Jackson and Hunt [26], changes λ. Mohanty [12] tried to measure the Soret coefficient in MnBi/Bi eutectic melts to determine whether if the effect would change the concentration distribution in the melt, and thus the spacing of the MnBi rods. To facilitate the development of a convection-free environment, Mohanty used small-diameter ampoules for his experiments. Since convection is governed by the Grashof number, and a decrease in ampoule diameter is directly proportional to a decrease in the Grashof number, a small ampoule diameter would help eliminate convection in the melt.

MnBi/Bi eutectic was placed in a temperature gradient (hot end at 700 or 750°C, cold end at 300°C) for a length of time, and then quenched with cold water. The ingot was sectioned and the Mn concentration measured by atomic absorption spectroscopy. Mohanty discovered that experiments with time durations of less than two days showed larger differences in concentration of Mn along the length of the sample when compared to experiments longer than two days in duration. In addition, he observed a separation of the components when the entire sample was exposed to 330°C for ten hours.

3. Theoretical Results

Effect of Convection on λ

Baskaran [7,46] studied the influence of convective flow on the lamellar spacing during directional solidification of eutectic alloys with a 50:50 composition. Considering a steady, well developed, laminar flow parallel to the solidification interface and perpendicular to the lamellae, he determined

the solute concentration in front of the growing interface using a numerical solution. From the numerical results, a correlation was obtained for the average interface undercooling. Baskaran then applied the extremum condition of Hunt and Jackson [26] to obtain a relation to predict the influence of convection on the lamellar spacing. He concluded that convection increases the lamellar spacing, and that the effect of convection increases as the lamellar spacing increases and as the diffusion coefficient decreases.

Following the same methods as Baskaran and Wilcox [7], Eisa [44] continued the theoretical study of the influence of convection on the microstructure of a lamellar eutectic, and extended the theoretical model of Baskaran and Wilcox to eutectic compositions of 10% and 30% and increased convection. He predicted that changes in λ should depend on the orientation of the lamellae with respect to the flow, with the maximum effect being when the flow is perpendicular to the lamellae. He speculated that the shift in lines of constant concentration should tend to make the lamellae grow in an upstream direction.

Eisa predicted that the change in λ should depend weakly on the eutectic composition, with the change being a maximum for a 50:50 volume fraction eutectic. He also predicted that λ should increase with increasing radial position when ACRT is used and the ratio of λ/λ_o depends almost entirely on the convective Peclet number $G_u\lambda_o^2/D$ and very little on the growth rate Peclet number $\lambda V/D$ for typical values of those variables. (Here G_u is the gradient of transverse velocity near the interface [s^{-1}], λ is the lamellar rod spacing, and λ_o is the lamellar rod spacing without convection [m], D is the diffusion coefficient in the melt [m^2/s], and V is the freezing rate [m/s].)

Caram et al. [8] developed a three-dimensional numerical model to study the influence of convection on a rod-like eutectic microstructure. By calculating the average melt concentration above the α and β solid phases using a central finite difference approach, they predicted that an increase in convection should coarsen the microstructure. This result is similar to those of Eisa [44], Chandrasekhar et al. [6,45], and Baskaran et al. [7,46] for lamellar eutectics. Caram et al. also determined that for the same intensity of convection, an increase in the eutectic composition increases the rod spacing, but the change due to convection is smaller for higher eutectic compositions. They also concluded that the direction of convective flow plays an important role in changing the rod spacing, since a flow in the y-direction provokes a bigger increase in rod spacing than a flow in the x-direction. Figure 5 is the geometry for the model developed by Caram et al.

In all the above numerical models developed to predict the effect of convection on the eutectic microstructure, a planar interface was assumed. However, Chandrasekhar experimentally showed that the interface of the MnBi/Bi eutectic is not planar; the rods of MnBi protrude beyond the Bi into the melt. Seth and Wilcox [13,47] developed a numerical model to study the effect of convection on the microstructure of a lamellar eutectic growing with a stepped interface as a semi-quantitative approximation for the rod eutectic. They concluded that increasing the intensity of convection increases the spacing between the lamellae and that the effect of convection is negligible if the flow velocity is very small in magnitude (convective Peclet number less than unity). They also concluded that for the same convective Peclet number, the microstructure of a stepped interface is more sensitive to convection than a planar interface. The eutectic is predicted to experience an increased change in the lamellar spacing due to convection as the interface becomes more irregular, but not to the extent of explaining the difference in λ for earth and space-processed samples.

Effect of Thermal Diffusion on λ

Caram and Wilcox [14] developed a mathematical model to describe the indfluence of the Soret effect during the growth of eutectic alloys. They formulated a differential equation describing the compositional field near the interface during unidirectional solidification of a binary alloy eutectic. This equation also included the contributions of both compositional and thermal gradients in the field.

The results of their analysis showed that the presence of thermal diffusion during rod eutectic solidification may change the fiber spacing, and that the change is due to a change in melt composition at the interface. However, they observed that the thermal diffusion coefficient for melts is generally very small compared to molecular diffusion, and that thermal diffusion has little affect on the rod spacing. Therefore, they found that the Soret effect is not enough to explain the change in rod spacing obtained from solidification in microgravity.

4. Comparison of Experiments and Theory

Effect of Composition on λ

Favier and deGoer [23] proposed an off-eutectic model to account for the influence of low gravity on eutectic spacing. Their model uses the Jackson and Hunt expression for off-eutectic (plane front) lamellar spacing written in terms of eutectic phase volume fraction [26,48]. Assuming the difference in λ for solidification on earth from that of low-gravity is due exclusively to the effect convection on the volume fraction, Favier and deGoer developed an expression relating the ratio of lamellar spacing at one-g and zero-g in terms of the volume fraction and characteristics of the phase diagram. Their derivation is detailed elsewhere [23]. Their model predicts a 30 to 50% difference between lamellar spacing at one-g and zero-g for a $\pm$ 1% deviation from the eutectic for a binary system with a very assymmetrical phase diagram. A positive deviation in composition was predicted to increase λ while a negative deviation should decrease λ. In the case of melts exactly at the eutectic composition, Favier and deGoer predicted that λ is unaffected by the influence of convection.

Barczy et al. [49], through their high gravity experiments with different Al_3Ni-Al alloys, concluded that the predictions of the Favier and deGoer [23] model seem invalid. To support this, Barczy et al. have found that λ changes monotonically with the concentration of Ni in their samples.

Effect of Convection on λ

Eisa et al. [9,44] obtained fairly good quantitative agreement between their experimental and theoretical results for the effect of spin-up/spin-down on λ, except at the lowest experimental freezing rate of 0.15 cm/hr where the microstructure was very irregular. They also concluded that convection coarsens the microstructure of the MnBi/Bi eutectic. For the quasi-regular fibrous microstructure formed at moderate to high freezing rates, the experimental results agree reasonably well with theoretical predictions [6-9].

Effect of Thermal Diffusion on λ

When samples were kept in a temperature gradient for at least 10 days, Mohanty [12] observed that his results were similar to those predicted by theory, but showed a much larger maximum concentration and much smaller minimum concentration of Mn. A comparison of the longer experiments to theoretical data indicated that the Soret coefficient was in the range of 1×10^{-8} to 5×10^{-8} $cm^2/C.s$, assuming a diffusion coefficient of 1×10^{-5} cm^2/s. However, since the only way to ensure a long-term, convection-free environment is to conduct experiments in microgravity, isolating the Soret effect in long-term ground-based experiments can prove to be a difficult, if not impossible task. Therefore, the fact that Mohanty observed a small value for the Soret effect may indicate that other mass-transport activity, such as microconvection and segregation due to gravity, affected the results of his experiments.

5. Conclusions and Future Work

The influence of a strong magnetic field during the solidification of the MnBi/Bi eutectic on earth has showed that reduced convection was the cause of the difference in microstructure of earth and space-grown samples [34]. However, 15 years of theoretical and experimental research have failed to reveal the mechanism for this phenomenon. Although the true mechanism has not been found, it has been determined that the temperature gradient has no effect on the microstructure of the MnBi/Bi eutectic [10], and that the Soret effect is not sufficiently large [12]. The microstructure adjusts to sudden changes in ampoule translation through the process of fiber branching and termination [11,31], and current interface demarcation was demonstrated as a feasible method for studying the solid/melt interface [29]. It was calculated that the concentration field in front of the freezing interface is not altered sufficiently by buoyancy-driven convection to explain the decrease in rod spacing, even if the MnBi fibers project out in front of the Bi matrix [6-8,45]. On the other hand, vigorous forced convection caused a change in microstructure in agreement with theory [6-9,44,45], and if it is assumed that the natural convection was underestimated by Baskaran and Wilcox [7], a reasonable explanation may be drawn to explain the fine microstructure seen in samples solidified in space.

To date, investigators at Clarkson and Grumman Aerospace have studied the unidirectional solidification of the MnBi/Bi eutectic in microgravity, under normal earth gravity, and in the presence of a strong magnetic field. Our future work will consist of studying the effects of high-gravity on the microstructure and the solid/melt interface of the MnBi/Bi eutectic.

These future plans are based upon the results of the high-gravity experimentation completed by Rodot et al. [50,51] in centrifuges located in France and the Soviet Union. They observed that samples of Ag-Doped PbTe solidified in a high-gravity environment have similar properties as that of samples solidified in space.

Further experimentation will include using current interface demarcation to study the changes, if any, in the interface of samples solidified in a high-gravity environment. Also, slightly off-eutectic samples will be solidified in normal and high-gravity to experimentally test Favier and deGoer's [23] hypothesis explained above in greater detail.

6. Acknowledgements

This research was supported by NASA grant NAG8-753.

7. References

[1] R.G. Pirich and D.J. Larson. In G.E. Rindone, editor, *Materials Research Society, Annual Meeting*, pg. 523, (1982).

[2] R. G. Pirich, D.J. Larson, and G. Busch, *AIAA J.* 19 (1981) 589.

[3] J. Bethin, "SPAR X Technical Report for Experiment 76-22. Directional Solidification of Magnetic Composites", Report RE-691, Grumman Aerospace Corporation, (1984).

[4] J.L. DeCarlo and R.G. Pirich, "Thermal and Solutal Convection Damping Using an Applied Magnetic Field," Report RE-680, Grumman Aerospace Corporation, (1984).

[5] R.G. Pirich and D. J. Larson, "SPAR VI Technical Report for Experiment 76-22. Directional Solidification of Magnetic Composites", Report RE-602, Grumman Aerospace Corporation, (1980).

[6] S. Chandrasekhar, G.F. Eisa and W.R. Wilcox. *J. Crystal Growth* 76 (1986) 485-488.

[7] V. Baskaran and W.R. Wilcox. *J. Crystal Growth* 67 (1984) 343.

[8] R. Caram, S. Chandrasekhar and W.R. Wilcox. *J. Crystal Growth* 106 (1990) 294-302.

[9] G.F. Eisa, W.R. Wilcox and G. Busch. *J. Crystal Growth* 78 (1986) 159-174.

[10] P.S. Ravishankar, Ph.D. Thesis, Clarkson University, (1980).

[11] W.R. Wilcox, K. Doddi, M. Nair and D.J. Larson, *Adv. Space Res.* 3 (1983), 79-83.

[12] A.P. Mohanty. M.S. Thesis, Clarkson University, (1990).

[13] J. Seth, M.S. Thesis, Clarkson University, (1990).

[14] R. Caram and W.R. Wilcox, "Influence of Convection on Microstructure," Third Semi-Annual Progress Report, NAG8-753, Clarkson University, (1990).

[15] F.R. Mollard and M.C. Flemings, *Trans. AIME* 239 (1967) 1534.

[16] F.R. Mollard and M.C. Flemings, *Trans. AIME* 239 (1967) 1526.

[17] G.A. Chadwick, *J. Inst. Metals* 92 (1964) 18.

[18] U.A. Tilles and R. Mrdjesovich, *J. Appl. Phys.* 341 (1963) 3639.

[19] A. Yue, *Trans. AIME* 224 (1962) 1010.

[20] P.S. Ravishankar, W.R. Wilcox and D.J. Larson, *Acta Met.* 28 (1981) 1583.

[21] C. Zener, *AIME Trans.* 167 (1946) 550.

[22] G. Muller and P. Kyr. In *5th European Symposium on Material Science Under Microgravity, ESA SP-222,* Schloss Elmau, W. Germany, (1984).

[23] J.J. Favier and J. de Goer. In *5th European Symposium on Material Science Under Microgravity, ESA SP-222,* Schloss Elmau, W. Germany, (1984).

[24] T. Carlberg and Y. Sayama, *J. Crystal Growth* 22 (1974) 259-271.

[25] A.S. Yue, B.K. Yue and J.G. Yu, *J. Crystal Growth* 54 (1981) 243-247.

[26] K.A. Jackson and J.D. Hunt, *AIME Trans.* 236 (1966) 1129.

[27] L.M. Hogan, F.D. Lemkey, and R.W. Kraft, *Adv. Material Res.* 5 (1971) 83.

[28] K.P. Doddi, M.S. Thesis, Clarkson University, (1981).

[29] T.W. Fu, Ph.D. Thesis, Clarkson University, (1981).

[30] T.W. Fu and W.R. Wilcox, *J. Crystal Growth* 48 (1980) 146.

[31] M. Nair, M.S. Thesis, Clarkson

University, (1981).

[32] B. Towloui and A. Hellawell, *Acta. Met.* 24 (1976) 565-573.

[33] D.J. Fisher, Ph.D. Thesis, Ecole Polytechnique de Lausanne, France, (1978).

[34] De Carlo, J.L., and Pirich, R.G., "Effect of Applied Magnetic Fields During Directional Solidification of Eutectic MnBi/Bi," Grumman Aerospace Corporation, (1984).

[35] H.P. Utech and M.C. Flemings, *J. Appl. Phys.* 37 (1966) 2021.

[36] H.A. Chedzey and D.T.J. Hurle, *Nature* 210 (1966) 933.

[37] D.J. Larson, Private Communication, (1991).

[38] R.J. Schaffer and S.R. Coriel, *Met. Trans.* 15A (1984) 2109.

[39] H.J. Scheel. *J. Crystal Growth* 13/14 (1972) 560.

[40] H.J. Scheel and E.O. Schulz-Dubois. *J. Crystal Growth* 8 (1971) 304.

[41] E.O. Schulz-Dubois. *J. Crystal Growth* 12 (1972) 81.

[42] P.Capper, J.J. Gosney, C.L. Jones and E.J. Pearce. *J Electronic Materials* 15 (1986) 361-370.

[43] P.S. Ravishankar, J.P. Dismukes and W.R. Wilcox. *J. Crystal Growth* 71 (1985) 579-586.

[44] G.F. Eisa. Ph.D. Thesis, Clarkson University, (1985).

[45] S. Chandrasekhar, Ph.D. Thesis, Clarkson University, (1987).

[46] V. Baskaran, M.S. Thesis, Clarkson University, (1983).

[47] J. Seth and W.R. Wilcox, *J. Crystal Growth,* In Press.

[48] J.D. Verhoeven and R.H. Homer, *Met. Trans.* 1 (1970) 3437.

[49] P. Barczy, J. Solyom, and L.L Regel, In *First International Workshop on Mateirals Processing in High Gravity,* Dubna, U.S.S.R., (1991).

[50] H. Rodot, L.L Regel, G.V. Sarafanov, M. Hamidi, I.V. Videskii and A.M. Turtchaninov, *J. Crystal Growth* 79 (1986) 77-83.

[51] H. Rodot, L.L. Regel, and A.M. Turtchaninov, *J. Crystal Growth* 104 (1990) 280-284.

Table 1: Summary of Microgravity Experiments on the MnBi/Bi Eutectic [9].

Flight Experiment	Freezing Rate	Temperature Gradient	Fiber Size and Spacing	Other Observations
ASTP	3 cm/hr	10 K/cm	2.5X Finer*	
SPAR VI	30 cm/hr	100 K/cm	3.0X Finer	7 v/o less*
SPAR IX	50 cm/hr	100 K/cm	2.0X Finer	Larger* Undercooling

*Than Samples Solidified on Earth

Table 2: Average Ratio of Rod Projection Length l to Rod Diameter d [20]

Growth Conditions	Avg. l/d	Std. Dev.	95%Conf. Limit
0.4 cm/hr with 100 rpm SU/SD	1.5	1.3	$\pm$0.55
3.0 cm/hr	1.5	1.3	$\pm$0.3
3.7 cm/hr	1.0	0.4	$\pm$0.053
3.7 cm/hr with 100 rpm SU/SD	1.9	2.6	$\pm$0.36
6.1 cm/hr	1.0	0	0

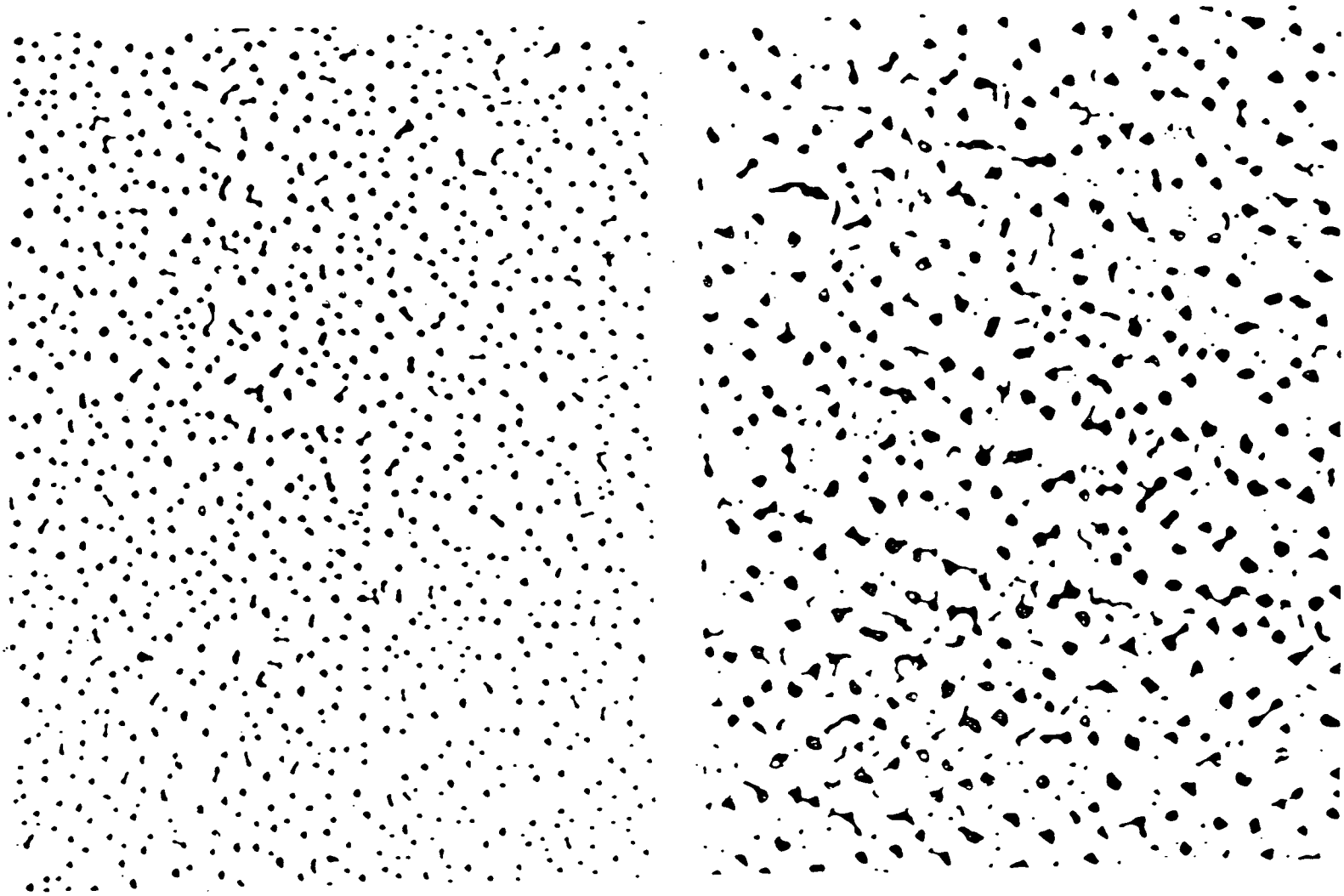

(a) (b)

Figure 1: MnBi/Bi Eutectic Solidified in Low Gravity (SPAR IX Sounding Rocket) (a), and a 1g Control Sample (b) [3].

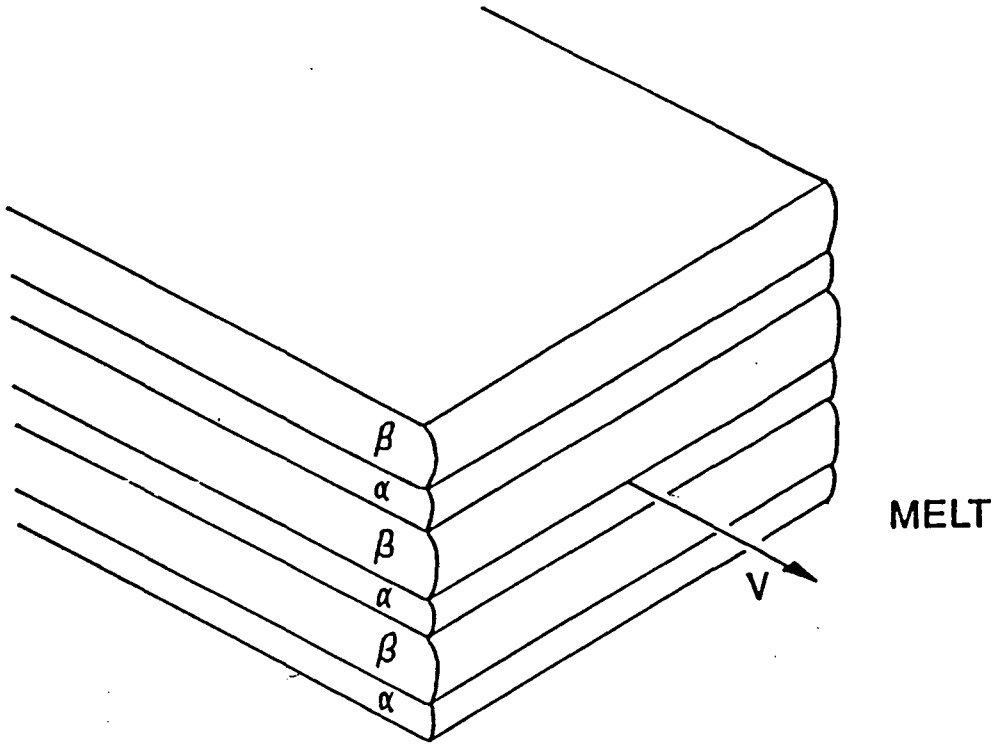

(a) Lamellar Growth of a Two Phase System.

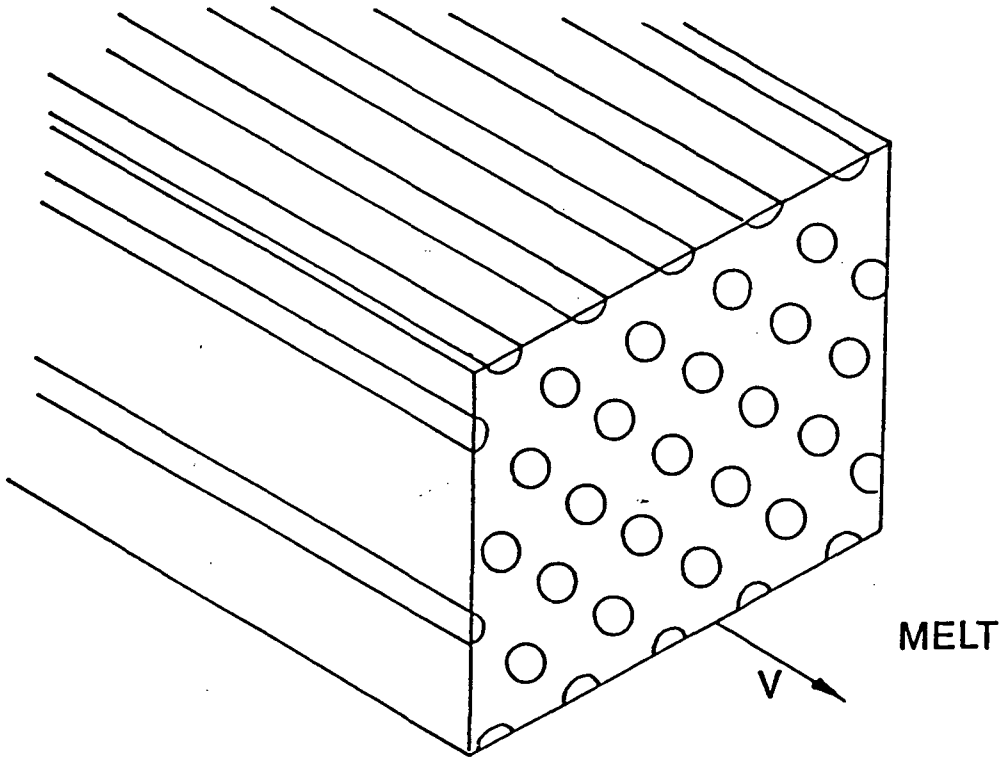

(b) Rod Growth of a Two Phase System.

Figure 2: Rod and Lamellar Growth of Two Phase System [41].

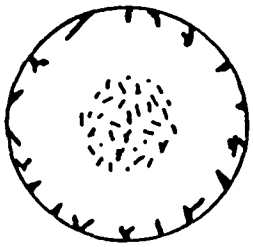

(a) 100 rpm su/sd, Hot Zone: 597 K, Cold Zone: 323 K, Core Dia.: 2.7 mm.

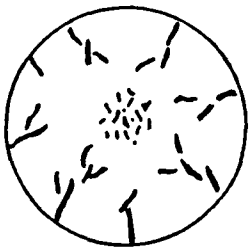

(b) 100 rpm su/sd, Hot Zone: 561 K, Cold Zone: 281 K, Core Dia.: 1.7 mm.

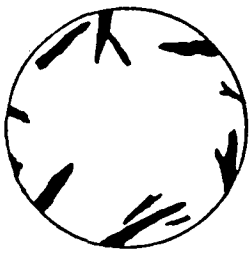

(c) 100 rpm su/sd, Hot Zone: 541 K, Cold Zone: 281 K, Core Dia.: none.

Figure 3: Schematics of MnBi/Bi Eutectic Microstructure With Spin-up/spin-down [20].

(a)

(b)

Figure 4: Decanted Interface of MnBi/Bi Eutectic Showing MnBi Rod Projection. Magnification: (a) 2.12 kX; (b) 1.83 kX [20].